Electron Transfer in Functionalized Fullerenes

by

Paul J. Bracher and David I. Schuster

a chapter (pages 163-212) in the book

Fullerenes: From Synthesis to Optoelectronic Properties

D.M. Guldi and N. Martín (editors)

Kluwer Academic Publishers (Dordrecht, The Netherlands)

2002

ELECTRON TRANSFER IN FUNCTIONALIZED FULLERENES

PAUL J. BRACHER AND DAVID I. SCHUSTER
New York University, Department of Chemistry
100 Washington Square East, New York, NY 10003

1. Introduction

A considerable amount of work concerning systems in which C_{60} is an electron acceptor has been published in the past three years, representing a substantial advance in knowledge over that summarized in the reviews published by Guldi and Kamat in 2000 [1] and by Martin *et al*. in 1998 [2]. Other reviews covering specific topics in this area have also appeared in the interim [3-5]. Accordingly, the present chapter will concentrate on new developments in this field, with only occasional reference to work published before 1999. The fundamental principles behind fullerene donor-acceptor systems are revisited and, for the first time, a section summarizing the experimental methods available for the study of these systems is presented. Other chapters in this volume deal with subjects that are very closely interwoven with the present discussion, specifically "Energy Transfer in Functionalized Fullerenes" (Armaroli), "Reorganization Energy in Functionalized Fullerenes" (Guldi), and "Photovoltaic Applications" (Hummelen). Where these subjects arise, as they will repeatedly, the reader will be referred to these chapters for more extensive discussions.

1.1. A CURIOUS NEW MOLECULE

The discovery in 1985 of buckminsterfullerene, C_{60}, by Kroto, Smalley, and Curl [6] marked the beginning of a new field in organic chemistry. The high degree of symmetry in C_{60} and in the arrangement of its molecular orbitals provides the foundation for a number of interesting chemical and physical properties. C_{60} is a good electron acceptor, and its triply-degenerate low-lying LUMOs (1.5–2.0 eV above the HOMO) allow for the reversible addition of up to six electrons [7]. Under mild conditions, the compound is relatively inert, which coupled with its negligible toxicity, has made functionalized fullerenes potential candidates for a variety of medicinal applications [8-10].

A great deal of research interest has been directed toward exploiting the photophysical and electrochemical properties of fullerenes. The ability of C_{60} to be reduced reversibly with up to six electrons has led to the synthesis of a large number of donor-acceptor systems in which it acts as an electron acceptor. While the ease of reduction of C_{60} has led to its extensive study as an electron acceptor, it is important to

note that C_{60} can also be oxidized, albeit with difficulty, by methods discussed in section 4.8. Remarkably small reorganization energies are associated with reductions of C_{60} and its derivatives, a trait that has led to the discovery of a number of cases [4, 11, 12] in which back electron transfer (charge recombination) occurs in the Marcus-inverted region [13-15]. The fact that charge recombination in these systems generally occurs more slowly than photoinduced electron transfer results in the generation of relatively long-lived charge-separated states. Thus, donor-acceptor systems containing fullerenes have been proposed as models for photosynthesis and as energy storage systems [5, 16, 17].

1.2. BASIC PHYSICAL PROPERTIES OF C_{60}

1.2.1. *Pristine C_{60}*

As stated previously, C_{60} can reversibly accept up to six electrons due to its triply-degenerate LUMO (t_{1u}), which lies 1.5–2.0 eV above its five-fold degenerate HOMO (h_u). The photophysical properties of pristine buckminsterfullerene have been previously reported and reviewed [3, 18-20]. C_{60} absorbs strongly in the UV and visible regions, with light of the longest absorption maximum at 620 nm effecting $h_u \rightarrow t_{1u}$ excitation of C_{60} to a singlet state. From the singlet excited state, intersystem crossing (ISC) to the lowest triplet excited state occurs with near unit efficiency. In aerated media, the C_{60} triplet excited state sensitizes the formation of singlet molecular oxygen ($^1\Delta_g$), whose growth and decay can be followed by monitoring its phosphorescence emission ($^1\Delta_g \rightarrow {}^3\Sigma_g^-$) at 1268 nm^{-1} [21]. In degassed solvents, triplet excited C_{60} has a limiting lifetime of 133 μsec and is deactivated by undergoing slow non-radiative decay back to the singlet ground state [22]. A faint fluorescence emission from the S_1 state of C_{60} at 703 nm ($\Phi_f = 1 \times 10^{-4}$) can be observed [23], but phosphorescence is too weak to be detected [24].

1.2.2. *Functionalized C_{60}*

Functionalized fullerenes often retain properties resembling those of the parent compounds, although there can be significant differences. Thus, monoadducts of C_{60} fluoresce at 698-703 nm with quantum yields similar to, although occasionally higher than, pristine C_{60} [25]. Most notably, C_{60} derivatives display reduction potentials that are cathodically shifted (require a greater negative potential) relative to pristine C_{60}, except when strongly electronegative atoms or moieties are bonded directly to the cage. Functionalized fullerenes are generally not able to display as many reversible reduction waves as pristine C_{60}, with some of them incapable of reversible reduction. In general, as the number of functional groups that are attached to the cage increases, the greater the likelihood there is for larger cathodic shifts in reduction potentials coupled with lower chances for reversibility.

Significant effort has been directed at the synthesis of functionalized fullerenes in which different chromophores or electroactive moieties are covalently-linked to the fullerene cage. In these systems, it is possible to reach the aforementioned excited and reduced states of the fullerene by indirect photophysical pathways [3], since activation or excitation of a linked chromophore can cause electron transfer (ET) or energy transfer (EN) to the fullerene to occur. While these molecules are sometimes difficult to

synthesize, they offer distinct advantages in such matters as molecular extinction coefficients in the visible region of the spectrum, the preference for population of singlet versus triplet excited states, and the ultimate fates (*i.e.*, lifetimes and reactivities) of these excited states.

1.3. FULLERENE DERIVATIVES FROM ORGANIC FUNCTIONALIZATIONS OF C_{60}

Early synthetic efforts were hindered by the fact that fullerenes were only available in limited amounts and also resisted many typical organic functionalization reactions. A process for the cost-effective mass production of fullerenes developed in 1990 by Krätschmer and Huffman [26] stimulated widespread fullerene research. In short time, it was found that the double bonds of C_{60} have similar reactivity to those of electron-deficient alkenes, and a large number of successful methods for the organic functionalization of fullerenes have since been discovered. These have made possible the synthesis of a large variety of molecules in which the properties of C_{60} can be modified and exploited [27-29]. C_{60} itself is usually the preferred fullerene substrate, as its high degree of symmetry relative to the other fullerenes leads to the possibility of fewer isomers upon functionalization. Most organic functionalization methods involve addition across the [6,6] double bonds, all thirty of which are equivalent in C_{60}. In more complex additions, where more than one double bond is attacked, certain *bis* and *tris* isomeric adducts are often preferentially formed [27-29]. In short, routine methods for the functionalization of fullerenes, coupled with the relatively simple isomeric mixtures obtained using C_{60} as the substrate, have allowed for the synthesis and subsequent photophysical study of a number of C_{60}-based materials. Corresponding derivatives of higher fullerenes have received much less attention.

2. Potential Applications of Photoinduced Electron Transfer Systems

2.1. MODELS FOR THE PHOTOSYNTHETIC REACTION CENTER (PRC)

In Nature, many plants and protozoa employ the biological process of photosynthesis to convert light into chemical energy [30]. This process takes place in chloroplasts, with the earliest events occurring within the recently characterized photosynthetic reaction center (PRC) in a few picoseconds [31]. Photosynthesis begins with the excitation of a chlorophyll molecule, followed by a series of electron transfer (ET) events in which a charge separated (CS) state is generated. The separated electrons are used to reduce $NADP^+$ to regenerate NADPH, which in turn reduces CO_2 to form simple sugars. As electrons "hop away" through the redox chain, the corresponding protons are pumped across thyalkoid membranes and used for the conversion of ADP into ATP. The early events have near 100% quantum efficiency, as energy-wasting charge recombination is reduced spatially by having the electron shuttled away a long distance from its point of origin, and kinetically by the low reorganization energy ($\lambda \sim 0.3$ eV) which forces charge recombination into the Marcus-inverted region [32]. The replication of these

two key properties has been the focus of research on artificial donor-acceptor systems designed to mimic the PRC [16].

2.1.1. *Main Objectives in PRC Mimicry Projects*

The early events in photosynthesis are characterized by high quantum yields and by negligible energy-wasting back electron transfer (BET). Due to a number of physical properties that will be discussed shortly, fullerenes have been effectively employed as electron acceptors in donor-acceptor systems designed to mimic the PRC. In donor-C_{60} systems in which the two chromophores are separated by short distances, very rapid ET usually occurs to the exclusion of EN, resulting in high quantum yields for formation of the CS state. Success has been obtained in attempts to lengthen the lifetime of the CS state by imitating the "electron hopping" in photosynthesis, which is effective at separating the electron from the donor moiety, such that energy-wasting recombination is inhibited. A general approach involves the utilization of a reduction gradient between the electron donor (D) and acceptor (A), by insertion of additional electroactive moieties between D and A. This strategy, which has been used in fullerene-containing systems [33, 34], makes it possible to create species in which the CS state ($D^{+\bullet}$–linker–$A^{\bullet-}$) is formed at distances where otherwise EN would be preferred. In these gradient systems, the electron "hops" away to the more distant acceptor as a consequence of an ET "cascade" in which it is energetically favorable for the excited electron to sequentially reduce adjacent moieties, as in Figure 1.

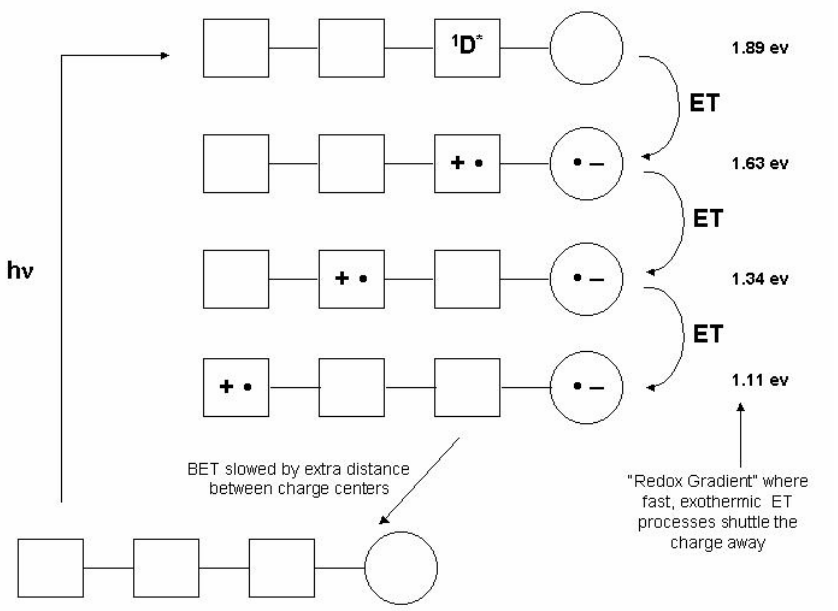

Figure 1. "Electron hopping" strategy to lengthen the lifetime of the charge separated states in a D–A system. Energy values for tetrad **28** [33].

An alternative strategy is to construct systems in which BET is retarded by reducing the reorganization energy (λ), which pushes BET into the inverted region of the Marcus parabola (Figure 2) describing the dependence of the rate of ET on the thermodynamic driving force [13-15]. This will be discussed later in greater detail.

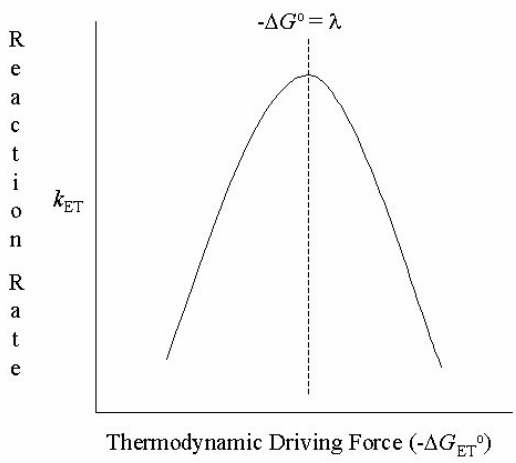

Figure 2. Marcus parabola for electron transfer processes

2.2. CONSTRUCTION OF ORGANIC PHOTOVOLTAIC CELLS

Tangentially related to the goal of mimicking photosynthesis by generation of long-lived CS states are attempts to construct photovoltaic cells in which light energy is used to generate an electric current. In such systems containing C_{60}, an organic donor chromophore is excited such that ET occurs and the fullerene is eventually reduced to the radical anion. When the donor and acceptor moieties are appropriately functionalized and attached to electrodes (anode and cathode, respectively), such that electrons can be transferred to and from the system, a photovoltaic cell results. For a more thorough explanation of these systems, the reader should refer to the chapter 11 by Hummelen in this volume.

2.2.1. *Main Objectives in Photovoltaic Cell Construction*

Many of the main issues affecting the utility of PRC mimics are shared by photovoltaic cells. The efficiency of charge separation and the reversibility of the ET processes are still important, as are several other factors. As photovoltaic cells are more ordered systems that involve solid-state as opposed to solution chemistry, the ease of cell fabrication becomes a particularly important factor. Coating metal and glass surfaces with thin films of the substrate is the most common method utilized for cell construction. The potential and current also become important qualities in judging cells, as any worthwhile system will have to produce electricity of satisfactory potential and be capable of pumping electrons at a quick pace.

3. Photophysical Pathways in C_{60} Derivatives and Methods for Their Study

3.1. EXPERIMENTAL METHODS

Although there are a wide variety of pathways available following photoexcitation of donor-acceptor systems containing fullerenes, a number of experimental techniques are available to determine which pathways are followed, to assess the extent each is preferred, and to measure the associated relative and absolute rates. There are also methods to probe the existence of ground state donor-acceptor interactions.

3.1.1. *Ultraviolet-visible (UV-vis) Spectroscopy*

UV-vis spectroscopy, which measures the extent of light absorption as a function of wavelength for a given sample, is a simple method for determining the presence of ground state interactions between the moieties in a hybrid system. In systems in which another chromophore has been covalently-linked to the C_{60} cage, the UV spectrum of the hybrid is usually the superposition of the spectra of the two components—those of a model C_{60} derivative and the attached chromophore. There are examples, however, in which bathochromic shifts are observed, indicative of ground state interactions between the π systems of the moieties [35-37].

Most functionalized fullerenes display a weak absorption band around 700 nm, although the exact cause of this absorption is still under debate [38]. If selective excitation of one chromophore over another is desired, UV-vis spectroscopy is useful in selecting the wavelength at which the hybrid system should be irradiated for subsequent photodynamic measurements. If possible, fullerene-containing hybrids are excited at wavelengths where there is a local minimum in the absorption spectrum of the fullerene moiety.

3.1.2. *Nuclear Magnetic Resonance (NMR) Spectrometry*

^{1}H and ^{13}C NMR Spectrometry. While most photophysical events occur on a timescale too fast for resolution by NMR, NMR can be a useful technique in assessing ground state donor-acceptor or $\pi-\pi$ interactions. The aromaticity of the fullerene cage generates ring currents that can influence chemical shifts of nearby protons, which provide clues as to their spatial proximity. For example, there have been reports of shielding of the internal hydrogens of porphyrin chromophores when these are located close to the fullerene cage [39, 40]. The same interaction can cause shifts in selected ^{13}C resonances on the fullerene sphere.

^{3}He NMR Spectroscopy. The deliberate incorporation of noble gas atoms within fullerenes was first achieved by Saunders *et al*. [41]. In the case of helium, the ^{3}He isotope has a nuclear spin and can be studied by NMR spectroscopy. In the last few years, ^{3}He NMR spectroscopy has been demonstrated to be a valuable tool in the study of fullerene derivatives [42-44]. While the chemical shift of the endohedral ^{3}He nucleus is known to be strongly affected by the extent and pattern of substitution on the fullerene cage, one can anticipate that ground state donor-acceptor and/or $\pi-\pi$ interactions should affect the magnetic field inside the fullerene and shift the ^{3}He resonance to higher fields. An illustration of the sensitivity of ^{3}He NMR as a probe for

such interactions is dyad **1**, in which the donor moiety (a porphyrin doubly-strapped to the C_{60} cage) shifted the resonance of the endohedral helium nucleus 0.4 ppm upfield relative to the functionalized fullerene lacking the donor group [45]. Interestingly, the UV-vis spectrum of this particular dyad gave no indication of intramolecular ground state electronic interactions. The sensitivity of this response suggests that the ^{3}He NMR technique deserves greater attention in this connection.

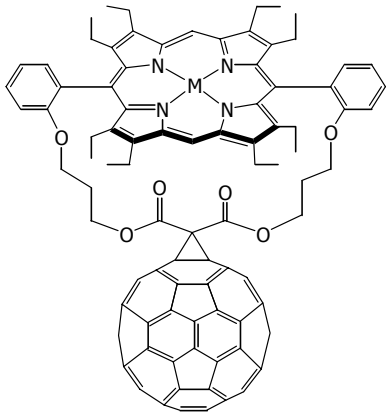

1a M = H_2
1b M = Zn

3.1.3. *Fluorescence Spectroscopy*

Fluorescence Quenching of Non-Fullerene Chromophores. A useful tool in assessing the degree of communication between the fullerene and donor moieties is the extent to which the fluorescence of the donor is quenched. This quenching process should be concentration independent if it is intramolecular in nature. An observation of fluorescence quenching is indicative of the activation of one or more competitive physical processes, most likely intramolecular electron or energy transfer.

C_{60} Fluorescence. While the overwhelming fate of singlet excited C_{60} is go undergo ISC to the triplet state, the slower competing process of fluorescence back to the singlet ground state can be observed at ~700 nm with a decay time on the order of 1.2 ns [3, 23]. If the fullerene moiety is selectively excited in the presence of a non-fluorescent donor moiety, the activation of EN or ET processes will cause quenching of fullerene fluorescence and a drop in the fluorescence lifetime [25, 46].

3.1.4. *Near-IR Spectroscopy/Singlet Oxygen Sensitization*

While triplet excited C_{60} ($^3C_{60}^*$) in degassed media slowly decays back to the ground state in a non-radiative process, in aerated media $^3C_{60}^*$ is quickly and efficiently quenched by ground state $^3O_2$ ($^3\Sigma_u$) to form $^1O_2$ ($^1\Delta_g$). The quantum yield for singlet oxygen formation following irradiation of C_{60} at 532 nm is 0.96 [18], and is only slightly smaller for monofunctionalized C_{60} derivatives [47-49]. Using an ultra-sensitive Ge-diode near-IR spectrometer, the generation of singlet oxygen can be

monitored by decay of its phosphorescence emission at 1268 nm [21]. Since $^3C_{60}^*$ generates singlet oxygen with near unit efficiency, formation of singlet oxygen is a useful experimental probe for the presence and yield of fullerene triplets on photoexcitation of hybrid systems.

3.1.5. *Cyclic and Differential Pulse Voltammetry*

Fullerene electrochemistry, while an important and interesting field in itself, is vital to understanding the photophysical processes in donor-acceptor hybrids [7, 50]. Through the techniques of cyclic voltammetry (CV) and differential pulse voltammetry (DPV), it is possible to derive the driving forces for charge separation ($-\Delta G^\circ_{ET(CS)}$) and for charge recombination ($-\Delta G^\circ_{ET(CR)}$) without having to probe short-lived transients produced upon irradiation. By sweeping an applied voltage to the compound in solution with a suitable electrolyte, the oxidation potentials (for donor moieties) and reduction potentials (for acceptor moieties) are measured. These values are plugged into the equations below [51] to obtain the thermodynamic driving forces for charge separation (CS) and charge recombination (CR):

$$-\Delta G^\circ_{ET(CR)} = e[E^\circ_{ox}(D^{+\bullet}/D) + E^\circ_{red}(A/A^{-\bullet})] \quad (1)$$

$$-\Delta G^\circ_{ET(CS)} = \Delta E_{0\text{-}0} + \Delta G^\circ_{ET(CR)} \quad (2)$$

The values of $-\Delta G^\circ$ are solvent dependent, as solvation of the charged species affects their stabilities relative to the ground state. The extent of solvent effects also varies greatly from compound to compound. These methods have been employed to determine the energies for CS states relative to electronic excited states and to construct Jablonski diagrams.

3.1.6. *Transient Absorption Spectroscopy*

While voltammetry measurements are useful in determining the relative energies of charge separated states, time-resolved transient absorption spectroscopy (TAS) is useful in measuring the kinetics of the population and decay of these states following an initial excitation pulse. For typical fullerene donor-acceptor hybrids, events occur typically in the nanosecond and picosecond time domains. Following initial excitation of a donor-acceptor hybrid, the absorption band for the C_{60} radical anion at 1000 nm will gradually grow in as electron transfer generates the charge separated state. Over time, the absorption will decrease as back electron transfer or other deactivation processes occur. From these data, the lifetime of the charge separated state can be determined.

It is also often possible to observe absorptions from other species generated upon excitation of the hybrid. For instance, radical cations of most zinc porphyrins ($ZnP^{+\bullet}$) display a transient absorption band around 650 nm. Thus, not only is it possible to measure the lifetimes of these species, but it is possible to discern the chronological sequence of events following photoexcitation.

3.1.7. *Charge Transfer Absorption*

Imahori and coworkers have recently reported the first charge transfer (CT) absorption and emission spectra of a porphyrin-C_{60} dyad [35]. The CT absorption band corresponds to excitation of the ground state into an excited state that possesses

extensive charge-separated character, much like an exiplex [52]. The spectrum is obtained by subtracting the UV absorption spectra of reference compounds for the D and A moieties from the UV spectrum of the D–A dyad in the same solvent at equal concentrations. A CT absorption band was observed only in the case of *ortho*-linked dyad **2** (λ_{max} = 721 nm, benzene; λ_{max} = 724 nm, PhCN), and not in *meta*- and *para*-linked analogues where there is less interaction between the D and A moieties. In the latter cases, the UV spectra of the dyads were simply the superposition of the separate moieties. A new fluorescence emission, attributed to the CT state, was also detected for **2** (λ_{max} = 810 nm, benzene), whereas other compounds in the series exhibited no emission at wavelengths besides those corresponding to the individual D and A chromophores. Surprisingly, CT emission was also detectable in benzonitrile, a very polar solvent. Typically, CT emission is observed only in nonpolar or weakly polar solvents. The Stokes shift of the CT emission from the absorption is roughly equal to 2λ, *i.e.*, twice the reorganization energy for the electron transfer process. Other electron transfer parameters can be derived using equations relating to Marcus theory [13-15]. This study shows that in cases where CT absorption and emission bands can be detected in D–A hybrids due to strong interaction between the chromophores, CT spectroscopy is a powerful tool to quantitatively determine ET parameters, such as the reorganization energy (λ) and the electronic coupling matrix element (*V*).

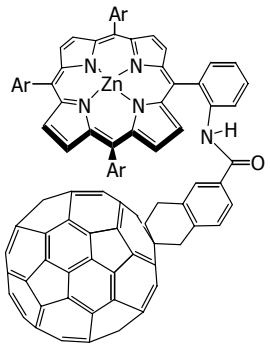

2

3.2. DESIGNING SYSTEMS FOR THE SELECTIVE ACTIVATION OF PATHWAYS

3.2.1. *What properties are desirable?*

There are many instruments and techniques available to study donor-acceptor systems and to extract physical values from these studies. The question then becomes what characteristics are desirable for potential practical application of these compounds, and how can researchers design hybrids to improve on these goals? The answer is not simple, as many factors influence the ultimate value of a hybrid system. Sometimes these beneficial factors are mutually exclusive—what is desirable in one hybrid is not necessarily desirable in another.

For instance, in the design of photosynthetic mimics, it is desirable to form long-lived charge separated states by increasing the rate of CS while retarding the rate

of energy-wasting BET. Efficiency is also a concern. In the case of developing compounds for the photosensitization of singlet oxygen, as for applications in photodynamic tumor therapy [53], increasing the propensity for EN to generate triplet excited C_{60} is desired. As EN competes with ET following excitation, either different hybrids must be used or the conditions of the experiment must be changed to achieve the desired result. There is also increasing evidence, however, that under certain circumstances, triplet states can be generated upon decay of CS radical pair states (see below).

3.2.2. *Factors Which Influence Pathway Selection*
While it is not yet possible to assess how changes in structure and reaction conditions will affect a hybrid's photophysical pathways *a priori*, there are a number of trends that have been observed which are summarized here. The main point is the extent to which conditions boost or hinder energy *versus* electron transfer, and to what extent each is favored in the competition.

Solvent. The selection of solvent greatly influences the relative energies of charge-separated states. Better solvation of CS states by increasing solvent polarity lowers the energy of these states, increasing the thermodynamic driving force for ET.

Donor-Acceptor Distance. The rate of ET varies as a function of distance to the inverse sixth power. Thus, the rate of ET rapidly falls off as the separation of the donor and acceptor moieties increases. This has been tested with donor-acceptor dyads bridged with variable-sized linkers.

Molecular Topology. It has been a long-standing goal of ET research to determine the effect on the dynamics of different molecular topologies, *i.e.*, how the donors and acceptors are connected and arranged in space. While a wide variety of hybrids have been synthesized and studied, many questions still remain. A useful tool in this study is modern molecular modeling software [54]. The influence of molecular topology on interactions between the π systems of porphyrin and fullerene moieties was recently investigated [55], and will be discussed in detail in section 4.2.1.

3.2.3. *Photophysical Switches*
Armaroli, Langa, Nierengarten and coworkers [56] have shown that by appropriate structural modifications and control of reaction conditions, one can selectively activate or deactivate EN and ET pathways in fullerene hybrids. This is discussed more fully in section 4.6.1.

4. Fullerene-Based Donor-Acceptor Complexes and Hybrids

This section will begin with a brief summary on intermolecular charge transfer complexes involving fullerenes as acceptors, and will continue with a discussion of molecular hybrids in which C_{60} is covalently linked or reversibly complexed with a variety of electron donors and ET is light-activated.

4.1. INTERMOLECULAR CHARGE TRANSFER COMPLEXES INVOLVING FULLERENES

Intermolecular photoreduction of C_{60} and C_{70} by excitation of the fullerene in the presence of a wide range of electron donors has been reviewed by Guldi and Kamat [1]. It has been shown that these involve electron transfer (ET) to C_{60} triplet excited states, as the rate of quenching correlates with the ionization potential of the donor.

Martín summarizes the literature up to 1997 on formation of charge transfer (CT) complexes between pristine C_{60} and a variety of electron donors, including tetrathiafulvalenes (TTFs), ferrocene, cobaltocene, decamethylnickelocene (DMN), and tetrakis(dimethylamino)ethylene (TDAE) [2]. In several of these systems, fully ionic electrically insulating CT complexes are formed, some of which are ferromagnetic. In the crystalline complex formed between C_{60} and DMN, the packing diagram clearly shows alternating nickel cations and C_{60} anions. Charge separation has also been observed in heterogeneous surfactant assemblies incorporating C_{60}, in which the fullerene triplet excited state is reduced by ascorbate [57, 58]. The long lifetime of the charge separated state (1–5 sec) is attributed to the spatial inhibition of reverse ET by the strong hydrophobic aggregation of the fullerene radical anions within the micelle, while the hydrophilic ascorbate radical cations remain in the aqueous phase. When a more hydrophobic electron donor which can better penetrate into the micelles was used, *e.g.*, 1,4-diazabicyclo[2.2.2]octane (DABCO), the lifetime of the charge separated state was reduced to 2.4 ms.

Due to the importance of intramolecular ET in dyads and larger molecular assemblies containing porphyrins and fullerenes (see below), it is important to first consider intermolecular electronic interactions between these moieties. Boyd *et al.* and Balch *et al.* reported that cocrystallates of fullerenes (C_{60} and C_{70}) and porphyrins (both free base and zinc-complexed) are formed by evaporation of equimolar solutions of these compounds in toluene or by other techniques [39, 59]. The X-ray structures of these naturally assembled cocrystallates indicate there is special attraction between fullerene and porphyrin moieties. The distances between the plane of the porphyrin and the closest atom in the fullerene range from 2.70 to 2.98 Å, which are shorter than expected for simple noncovalent interactions. For example, π–π interactions in fullerene/arene and porphyrin/arene systems lead to separations in the range of 3.0–3.5 Å. In the tetraphenylporphyrin (H_2TPP)–C_{60} crystal, the electron-rich center of H_2TPP is situated directly over a [6,6] bond in C_{60}, *i.e.,* an olefinic bond shared by two six-membered rings. This is attributed to electrostatic attraction between the electron-deficient center of the porphyrin and the electron-rich [6,6] bond of the fullerene. Slightly distorted structures were seen in some of the other C_{60}-cocrystallates, although the center of the porphyrin (metallated or not) is as close as possible to a fullerene [6,6] bond. In the C_{70} structures, the fullerene carbons closest to the porphyrin are those at the most electron-rich site, namely the intersection of three fused six-membered rings. In no cases were close fullerene-fullerene contacts observed. Boyd *et al.* performed molecular modeling studies on the fullerene-porphyrin clusters, which gave the same kind of alternating porphyrin/fullerene zig-zag chains and intermolecular separations as observed in the X-ray structures. Significant interaction energies (28.0–33.6 kcal/mol) for both C_{60} and C_{70} with H_2TPP were calculated using Universal and PCFF force fields

[39]. In all cases, the major contribution (80-95%) to the total binding energy came from the van der Waals and not the electrostatic terms of the force field. Similar interactions in the solid state have been reported between C_{60} and octaethylporphyrins and porphyrazines [59-61]. Using ESFF and CVFF force fields, these observations [39] have been exactly reproduced computationally [54].

As far as porphyrin-fullerene electronic interactions in solution are concerned, Boyd *et al.* [39] noted that the UV-vis spectra of an equimolar solution of C_{60} and tetraarylporphyrins are simply the sum of the spectra of the individual chromophores, a finding which is reproduced in most of the analogous studies on covalently-linked dyads discussed below. It must follow that either electronic spectroscopy is insensitive to complex formation or that the degree of association is weak. However, small upfield shifts of the nearest nuclei in the X-ray structures are observed in the fullerene ^{13}C and the porphyrin (N-H) ^{1}H NMR spectra of the mixtures, indicative of complex formation. In summary, while distinct intermolecular charge-transfer complexes apparently are not formed between porphyrins and fullerenes, association of these species is a real supramolecular phenomenon, primarily attributed to favorable van der Waals attraction between the planar surface of the former and the curved surface of the latter. This type of interaction plays a major role in the photophysics of dyads in which these two moieties are covalently linked [54].

4.2. INTRAMOLECULAR PHOTOINDUCED ELECTRON TRANSFER AND THE PROPERTIES OF CHARGE-SEPARATED STATES IN DYADS, TRIADS, AND LARGER MOLECULAR ASSEMBLIES AND COMPLEXES CONTAINING FULLERENES AND PORPHYRINS

Since the greatest amount of work on photoinduced electron transfer (PET) in donor-acceptor dyads, triads, and larger assemblies has been done on systems in which the fullerene (acceptor) is covalently linked to a porphyrin (donor) by a variety of rigid, semirigid, and flexible spacers, this subject will be discussed first. Recent work has revealed the very strong dependence of the rates of forward and back ET on molecular topology, substituents on the porphyrin ring system, incorporation of metals inside the porphyrin, and solvent polarity. These same factors, most crucially the polarity of the solvent, also affect the competition between PET and EN. In almost all cases, by appropriate choice of wavelength, the porphyrin can be selected as the principal light-absorbing species.

We will focus on systems that have been constructed within the past two years, with limited discussion of earlier literature. If no new data is available on compounds discussed in the earlier reviews, the compounds will be omitted from the discussion, unless the old data bears directly on interpretation of newer data or has historical significance.

4.2.1. *Fullerene-Porphyrin Dyads*

The first published report in this field in 1994 by the Arizona State team headed by Gust, Moore, and Moore (hereafter designated GMM) concerned dyad **3** and established some of the important ground rules for this field [40]. Using techniques discussed in section 3.1, it was shown that (a) excitation of the free base dyad **3a** ($P–C_{60}$) to give

$^1P^*$–C_{60} is followed by singlet-singlet EN in a nonpolar solvent (toluene) to give P–$^1C_{60}^*$, (b) in benzonitrile, PET to give $P^{+\bullet}$–$C_{60}^{\bullet-}$ competes with EN, (c) in toluene P–$^1C_{60}^*$ undergoes typically efficient (for C_{60}) intersystem crossing to P–$^3C_{60}^*$, but in benzonitrile ET occurs to give the analogous charge-separated state $P^{+\bullet}$–$C_{60}^{\bullet-}$, and (d) the corresponding Zn complex (ZnP–C_{60}) in both toluene and benzonitrile undergoes only very rapid ($k_{ET} \sim 10^{11}$ s^{-1}) PET to give the charge separated state. The differences in the processes induced by photoexcitation of P–C_{60} as a function of solvent and of P–C_{60} *vis à vis* ZnP–C_{60} were rationalized in terms of the energies of the various intermediates, namely $^1P^*$–C_{60}, P–$^1C_{60}^*$, P–$^3C_{60}^*$ and $P^{+\bullet}$–$C_{60}^{\bullet-}$.

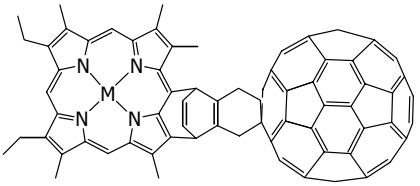

3a M = H_2
3b M = Zn

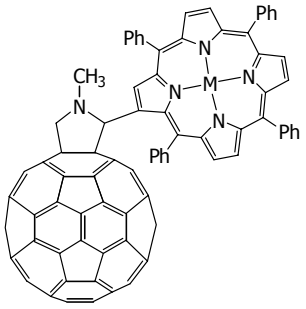

4a M = H_2
4b M = Zn

Similar results were reported by GMM and coworkers for dyad **4** [46]. Specifically, it was shown that for the free base dyad **4a** in toluene, charge separation is not observed from either $^1P^*$–C_{60} or P–$^1C_{60}^*$, while in benzonitrile PET competes with PEN, just as with **3a**. For the corresponding Zn dyad **4b**, PET is seen in toluene as well as benzonitrile. The lifetime of the CS state was 290 ps in the case of **4a** and 50 ps in the case of **4b**. Thus, charge recombination in these systems is very rapid, although somewhat slower than charge separation. According to molecular modeling studies using Insight II and Discover, dyads **3** and **4** adopt a folded conformation in which D_{cc}, the distance from the center of the P moiety to the center of the C_{60}, is 9.9 Å. The endergonic free energy changes for formation of $P^{+\bullet}$–$C_{60}^{\bullet-}$ and $ZnP^{+\bullet}$–$C_{60}^{\bullet-}$ were estimated at 0.58 eV and 0.37 eV, respectively.

Similar studies were carried out by GMM on the analogous octaalkylporphyrin dyad **5** [62]. In general, the pattern of behavior was very similar to that of dyad **4**, with one significant difference. Excitation of the P moiety in toluene gives $^1P^*$–C_{60} which very rapidly (11 ps) decays to the CS state $P^{+\bullet}$–$C_{60}^{\bullet-}$, detected by transient absorption experiments. Decay of this species (τ = 1.25 ns) is directly correlated with formation of the lower-lying singlet excited state of the fullerene, P–$^1C_{60}^*$, indicating that in toluene the CS state of **5** lies energetically between the lowest lying P and C_{60} singlet excited states, an unusual but not unique occurrence. The small driving force of ~ 0.1 eV for charge recombination to give P–$^1C_{60}^*$ places this process in the normal region of the Marcus curve, while decay to the ground state of the system with ΔG^o = -1.84 eV is in the inverted region and therefore occurs much more slowly [62]. As expected, P–$^1C_{60}^*$ in turn undergoes unperturbed intersystem crossing with unit efficiency to give P–$^3C_{60}^*$,

which in turn decays to the ground state with a lifetime of 90 μs. In the more polar solvent benzonitrile, P–$^1C_{60}^*$ is accessible only by an EN pathway, and is rapidly quenched by ET from ground state P to give the lower lying CS state (driving force 0.31 eV) at a rate of 3.1 x 10^{10} s^{-1}.

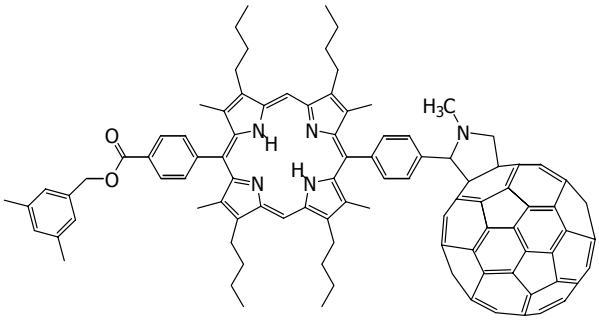

5

Studies by Imahori, Sakata, Ito, Fukuzumi, and coworkers have focused on the role of molecular topology on the photophysics of fullerene-porphyrin dyads [63]. This is illustrated by dyad **6** in which a *meso*-phenyl group on the porphyrin ring (the other three *meso* positions are occupied by 3,5-di-*tert*-butylphenyl groups which improve solubility in common organic solvents) is linked at the *para* position by an amide moiety to the *meta* position of another phenyl group, appended to a six-membered ring attached to C_{60}.

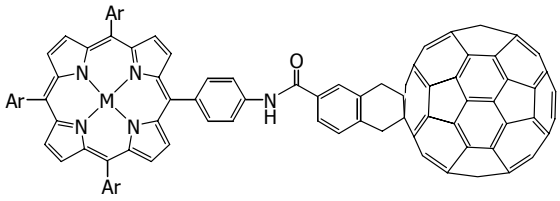

6a M = H_2
6b M = Zn

Variations on this structure were studied in which the linkage to the *meso* phenyl is changed to *ortho* and *meta*, and in which the linkage on the phenyl appended to the fullerene is changed from *meta* to *ortho*. In these systems, the center-to-center distance between the P and C_{60} moieties in folded conformations is subtly varied. While there are some differences in these systems, the overall pattern is very similar [63]. For the Zn dyads (ZnP–C_{60}) in THF, very rapid ET occurs upon excitation of either P or C_{60} to give a charge-separated (CS) state, $ZnP^{+\bullet}$–$C_{60}^{\bullet-}$, which decays at a slightly lower rate back to the ground state. For the same dyads in benzene, PET to give the CS state is still rapid, but since this state is of higher energy, it is in equilibrium with ZnP–$^1C_{60}^*$. The rate for charge recombination in **6b** is decelerated relative to an

analogue with a two-dimensional acceptor (benzoquinone) in place of the fullerene [64]. The authors propose that the total reorganization energy (including intramolecular (λ_i) and solvent (λ_s) contributions) for ET involving C_{60} is relatively small, which is apparently the first mention of this important effect (see below) in the fullerene ET literature. They refrain, however, from proposing at this point that back electron transfer actually occurs in the Marcus "inverted region." Very little work has been reported on the corresponding free base dyad **6a** and the free bases of the structural variants described above. In the case of **6a**, transient absorption attributable to $P^{+\bullet}$–$C_{60}^{\bullet-}$ is not observed, but instead broad structureless transient absorption ascribed to an "intramolecular exciplex" is seen. No details or spectra were provided [17].

As discussed in section 3.1.7, Imahori, Fukuzumi, and coworkers [35] showed that the *ortho*-linked Zn complex **2** displays both charge transfer (CT) absorption and fluorescence emission spectra. No such difference is seen for the corresponding *meta*- and *para*-linked dyads (**6b**), indicating that very close contact between the P and C_{60} moieties, *i.e.* π-stacking, is essential for the observation of CT absorption. Analysis of the fluorescence data using Marcus theory [13-15] allowed the authors to determine the parameters associated with back electron transfer (BET) in benzene, namely the reorganization energies λ_v (0.10 eV) and λ_s (0.13 eV) and the free energy for back electron transfer, $-\Delta G^{o}_{BET}$ (1.66 eV). The latter was in fair agreement with the value of 1.39 eV calculated from electrochemical data, which may be slightly lower due to the high concentration of the electrolyte. The very small total reorganization energy, $\lambda = 0.23 \pm 0.11$ eV, is also consistent with the Stokes shift between the CT emission and absorption spectra. Most importantly, the value of λ is the smallest ever reported for inter- or intramolecular synthetic donor-acceptor systems, and is comparable to the smallest values measured for the photosynthetic reaction center [14, 32, 65]. This demonstrates conclusively that intramolecular charge separation in fullerene-porphyrin systems in solution can mimic photosynthetic charge separation in the absence of the protein environment required in the latter system. For further discussion of this point, see chapter 9 by Guldi in this volume.

A series of P–C_{60} dyads with flexible polyether linkers have been synthesized in a convergent manner by the NYU group [66, 67]. In the first two examples (see structures **7** and **8**), the basic characteristics of these types of systems were established. Firstly, for **7a** and **7b**, small bathochromic shifts (6-10 nm) are seen in the UV-vis spectra compared with the corresponding porphyrin methyl ester in nonpolar (benzene) as well as relatively polar (CH_2Cl_2) solvents (interestingly, no such effects were seen for **8**). Secondly, porphyrin fluorescence is significantly quenched (70-80%) in benzene and 1:1 benzene-methanol. Thirdly, these dyads are reasonably good photosensitizers for O_2 ($^1\Delta_g$) formation (solvent: 2:1 benzene-d_6/CD_3OD or acetone-d_6), with quantum yields of 0.10, 0.21 and 0.40 relative to that of tetraphenylporphine ($\Phi_\Delta = 0.62$) upon excitation at 532 nm [68, 69]. Although fluorescence lifetime and transient absorption data have not been obtained on these compounds, it is clear that P–$^3C_{60}^{*}$ must be formed, at least in nonpolar solvents. Whether this is by an EN pathway or by CR from CS states remains to be established. The fact that fluorescence quenching is greater in the more polar solvent suggests that PET occurs, but no definitive conclusions regarding PET can be reached without transient absorption data. Based upon the earlier discussion, the P and C_{60} moieties should be in close proximity in these flexibly linked

dyads, which was not recognized at the time this work was originally done (1996-97). The spectral shifts and strong fluorescence quenching are in accord with this hypothesis. Additional support came from ^{3}He NMR data for dyad **7a** prepared from ^{3}He@C_{60}, where the ^{3}He resonance was 0.9 ppm upfield from that of the fully functionalized fullerene lacking the P residue [70]. As suggested earlier, ^{3}He NMR is probably the best probe for ground state electronic interactions in P–C_{60} hybrids, although this novel technique has thus far been used only sparingly in this context (see section 3.1.2).

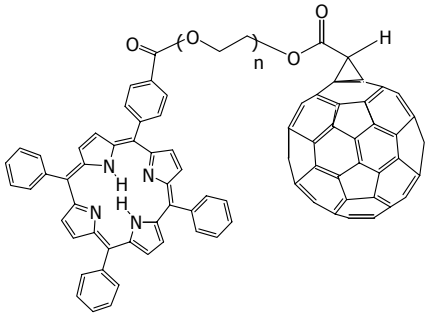

7a n = 4
7b n = 5

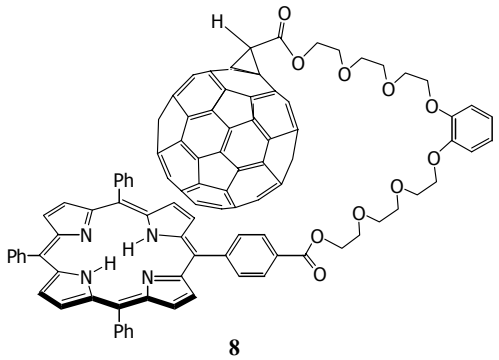

8

The later finding that fluorescence quenching in dyad **9** (see below) is much greater than in **7** and **8** indicates that the P–C_{60} intramolecular interactions in **7** and **8** are probably not optimal. Indeed, it is possible to improve such interactions in **7** by formation of metal ion complexes with the pseudo crown ether linker, as predicted by molecular modeling studies [66]. The computations suggested that complexation of K^+ should be particularly effective in bringing the P and C_{60} chromophores closer together. Substantial spectral shifts were observed in the UV-vis spectrum of **7a** upon the addition of KSCN, which also enhanced quenching of the residual porphyrin fluorescence. No effect of adding K^+ salts on the spectral properties of porphyrin model compounds or dyad **8** was observed, indicating that these unusual effects depend on the size and topology of the linker. Thus, such salt effects should be observed only for those systems in which (a) the P and C_{60} moieties are not already optimally aligned, and (b) where binding of the metal to the linker can effectively alter the topological relationship of the two chromophores in the dyad.

Analogous P–C_{60} dyads **9a** and **9b**, in which the C_{60} synthon has been changed for synthetic convenience while the tri- and tetra-ethylene glycol linkers have been retained, have been prepared and subjected to extensive photophysical study [71]. As indicated earlier, quenching of the P-derived fluorescence is much greater in **9** than with **7** and **8**. Molecular modeling studies [54] suggest very close approach of the P and C_{60} moieties is possible in **9**, with separation distances between the chromophores on the order of 2.64 Å. Transient absorption studies confirm that CS states are formed in all five solvents studied, ranging in polarity from toluene to DMF, with rate constants (k_{CS}, obtained from growth of $C_{60}^{\bullet-}$ absorption) ranging from 4.5 x 10^8 s^{-1} to 1.2 x 10^{10} s^{-1} and quantum yields (Φ_{CS}) between 0.19 and 0.67 (See Table 1). There is no simple correlation between Φ_{CS} and solvent polarity, suggesting the solvent is playing more

than one role. The rate constants k_{CS} increase as solvent polarity increases, indicating that ET occurs in the normal (*i.e.*, uphill) portion of the Marcus curve. Since the CS state is stabilized in polar solvents relative to the ground state of the dyad, the thermodynamic driving force for charge recombination ($-\Delta G^{o}_{CR}$) is greater in less polar solvents. The fact that k_{CR} increases as solvent polarity is increased (*i.e.*, the lifetime of the CS state is greater in nonpolar *vis à vis* polar solvents) can only be understood if CR is occurring in the Marcus "inverted region," which is reasonable given the relatively small reorganization energy associated with fullerenes in ET processes [3, 4, 12, 35, 64]. The finding that **9a** and **9b** act as photosensitizers for $^1O_2$ formation in both toluene (Φ_{rel} = 0.34 for both) and benzonitrile (Φ_{rel} = 0.18 and 0.09, respectively) implies that C_{60} triplet states are being generated, but it is not possible from the data to differentiate between two alternative mechanisms, namely singlet-singlet energy transfer (EN) followed by intersystem crossing (ISC) and BET from the CS state. Both mechanisms have precedent [12, 40, 46, 62, 72, 73].

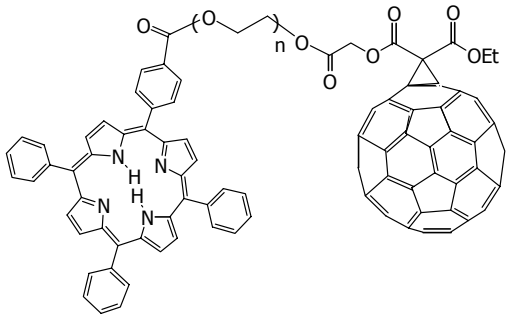

9a n = 3
9b n = 4

TABLE 1. Photophysical data regarding ET and BET in dyads **9a** and **9b** in various solvents.

	Dyad **9a**			Dyad **9b**		
Solvent	k_{ET} $(ns)^{-1}$	τ_{CS} (ns)	Φ_{CS}	k_{ET} $(ns)^{-1}$	τ_{CS} (ns)	Φ_{CS}
Toluene	5.32	373	0.19	4.50	396	0.33
THF	6.90	288	0.24	6.02	298	0.34
o-DCB		246	0.50		270	0.67
Benzonitrile	11.1	115	0.37	10.1	156	0.43
DMF	12.0	83	0.17	10.5	99	0.19

Guldi and coworkers have recently reported extensive photophysical data on two π-stacked P–C_{60} dyads **10** and **11**, which possess the same linkers but differ significantly in molecular topology [55]. In the C_2-symmetric dyad **10**, there is a *trans*-2 linkage of the Zn tetraryl porphyrin (ZnTPP) moiety to C_{60}, whereas in dyad **11** the macrocycle containing the ZnTPP bridges between two equatorial positions [28]. The double linkage enforces a face-to-face orientation of the two chromophores in **10**, as compared with an edge-to-face alignment in **11**. This difference turns out to have a

profound effect on the photophysics of these two conformationally rigid systems. For both, Φ_f (ZnTPP) is strongly quenched, accompanied by rapid growth of transient absorption characteristic of $P^{+\bullet}$ and $C_{60}^{\bullet-}$ in solvents ranging in polarity from toluene to DMF. The only exception is **11** in toluene, where EN prevails. In the case of **10**, the rise time for formation of the CS state by PET is within the response time of the instrument, *i.e.*, < 35 ps. In the case of **11**, however, this process is slower by a factor of 10. While the values of $-\Delta G^{o}_{ET}$ for dyads **10** and **11**, determined from spectroscopic and electrochemical data, are not very different, values of the electronic coupling matrix element *V*, a critical parameter in determining rates of electron transfer, are much larger for **10** than for **11**, according to semiempirical MO calculations. This is a consequence of the very effective π–π stacking in **10** which is not possible in **11**. Observed spectral shifts in the case of **10** are consistent with strong π–π interactions.

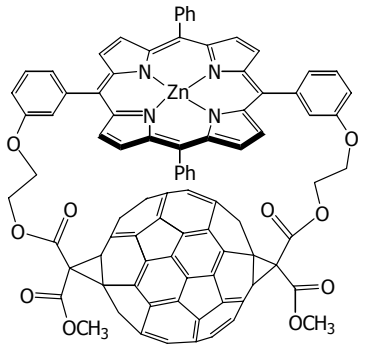

10

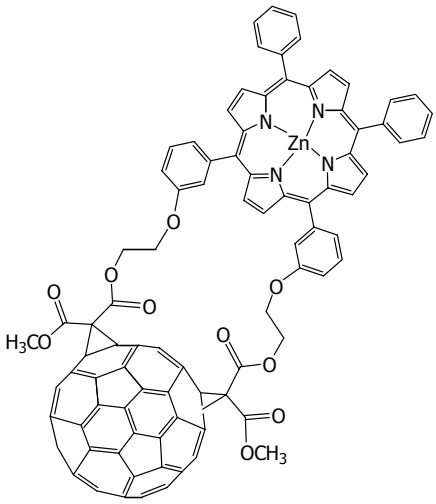

11

The most striking difference between the two systems is in the rates of back electron transfer, *i.e.*, k_{CR}, which are slower by about four orders of magnitude for **11** compared to **10** [55]. This is directly attributable to the change in alignment of the two chromophores. Nonetheless, for both dyads, the variation in k_{CR} with solvent polarity, *i.e.*, with the thermodynamic driving force $-\Delta G_{CR}^{o}$, is consistent with charge recombination occurring in the Marcus inverted region. Thus, the lifetime of the CS radical pair for **10** decreases from 619 ps in toluene to 38 ps in benzonitrile. The possibility that the solvent is playing a direct role in mediating back electron transfer, particularly in the case of **11**, cannot be excluded.

A different tack was taken by Schuster, Cheng and Wilson, who prepared P–C_{60} dyad **1** in which a cyclophane linkage would presumably constrain the planar P surface to lie directly above the fullerene sphere, to promote intramolecular electronic interactions [45]. As opposed to the case of **10**, in which *bis*-addition to C_{60} holds the two chromophores in place, in **1** there is only a single site of attachment to C_{60}, which

provides minimal perturbation of the electronic properties associated with the fullerene moiety. Synthesis of **1** was achieved by a Bingel-Hirsch reaction on a macrocylic malonate tied to either end of a 5,15-diaryl porphyrin derivative. Until recently, it was believed that the conformation of **1** was the structure shown in Figure 3b with C_{2v} symmetry, resembling a parachute. Photophysical studies of **1** [12, 74] showed that PET to give a CS state indeed occurred very rapidly for the free base as well as the ZnP systems, at rates approaching 10^{11} s^{-1}, in a variety of solvents ranging in polarity from toluene to DMF. Although CR occurred rapidly, $k_{CR} \sim 10^{11}$ s^{-1}, k_{CR} is still an order of magnitude smaller than k_{CS} (see Table 2). This, together with the fact that k_{CR} increased with increasing polarity of the solvent (*i.e.*, the lifetime of the CS state was inversely proportional to solvent polarity), strongly suggested again that BET for **1** is in the Marcus inverted region [12]. Transient absorption and $^1O_2$ ($^1\Delta_g$) sensitization studies showed that BET from the CS state in toluene led to fullerene triplet states ($P–^3C_{60}^*$) with a quantum efficiency of about 0.2. Fullerene triplets were not formed in other solvents, or from the Zn dyad in any solvents, indicating that only for the free base dyad in toluene does the CS state lie energetically above $P–^3C_{60}^*$. In these respects, the photophysics of **1** are not very different from those of analogous dyads discussed earlier.

TABLE 2. Lifetime of the CS state of dyad **1** in various solvents.

	τ_{CS} (ns)	
Solvent	**1a**	**1b**
THF	0.314	0.099
CH_2Cl_2	0.232	0.095
o-DCB	0.201	0.095
Benzonitrile	0.155	0.069
DMF	0.107	0.056

The question arises of the conformational flexibility of "parachute" dyads such as **1**, and how this impacts on its photophysical properties, relative to the structure and properties of more rigid dyads such as **10** and **11** [55]. This problem has been recently addressed computationally [54]. Indeed, for **1** and a large number of analogous "parachute" dyads with varying porphyrin substitution patterns, linker sizes and positions of attachment to the porphyrin core, the most stable structure predicted in every case is that in which the P moiety swings over to the side of the C_{60} sphere. In this unsymmetrical conformation, illustrated for the case of **1** in Figure 3a, the center-to-center distance (D_{cc}) is substantially less (~ 6.5 Å) than that (~ 10 Å) associated with the C_{2v} structure in Figure 3b. This is an additional illustration of the importance of the attractive van der Waals forces between porphyrins and fullerenes, discussed earlier [39, 59]. The ^{3}He NMR spectrum of **1** prepared from $^3He@C_{60}$ shows an upfield shift of 0.4 ppm relative to an appropriate fullerene derivative lacking the porphyrin moiety, which is indicative of significant ground state π–π interaction in this dyad.

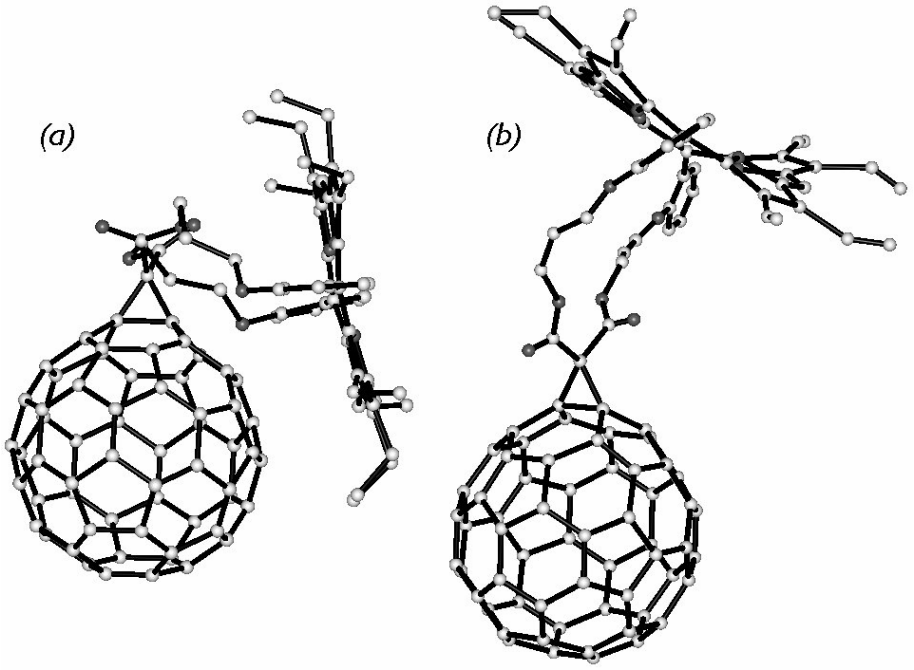

Figure 3. Unsymmetrical "compact" (a) and C_{2v} "extended" (b) molecular modeling structures of dyad **1**

Since the ^{1}H NMR spectrum of **1** is in accord with a symmetrical dyad structure, it appears that the dyad is conformationally mobile at ambient temperatures, swinging back and forth between the two lowest energy conformations through the higher energy symmetrical structure [54]. The rate of PET for **1** is about the same as for **10**, suggesting that this process in **1** is probably occurring in the unsymmetrical conformation, where the center-to-center distance is minimal. Synthesis and photophysical studies of analogous "parachute" dyads which are predicted to be conformationally either more or less rigid than **1**, along with variable temperature ^{1}H NMR studies, should be particularly informative. The computations suggest that it should be possible to tune the rates of charge separation, since k_{CS} should correlate with the computed D_{cc} value through the electronic coupling matrix element *V*. A correlation between k_{CR} and D_{cc} has yet to be established.

An attempt to achieve the opposite goal, namely to force the P and C_{60} moieties far apart, was made using a steroid linker to separate the chromophores. Using methodology adapted from that used by Maggini, Guldi and coworkers [75] to prepare analogous $[Ru(bpy)_3]^{2+}$ dyads, androstan-3-one was first linked to C_{60} by a Prato reaction, and the P moiety was then attached at the other end to give **12** [76]. This synthesis was repeated with two other steroids. In this synthesis a new stereogenic center is created, with *R* and *S* configurations at the spiro carbon atom. In the *R* epimer, the angular methyls on the steroid point toward the C_{60} while in the *S* diastereomer, they point away; this is also true in the steroid-linked $[Ru(bpy)_3]^{2+}$–C_{60} dyads [75]. ^{1}H NMR

spectra suggested both diastereomers were present. Subsequent photophysical studies of **12** and the other steroid-linked dyads, performed on the mixture of diastereomers, showed that the porphyrin fluorescence was significantly quenched (52-71% in benzene, 66-74% in $CHCl_3$); the compounds were also found to be excellent $^1O_2$ ($^1\Delta_g$) sensitizers. More recent transient absorption studies on **12** indicate the formation of relatively short-lived CS states in all solvents studied with the exception of toluene. The rise time for formation of these states is on the order of 500 ps, considerably longer than in the cases of **1**, **9**, **10**, **11**.

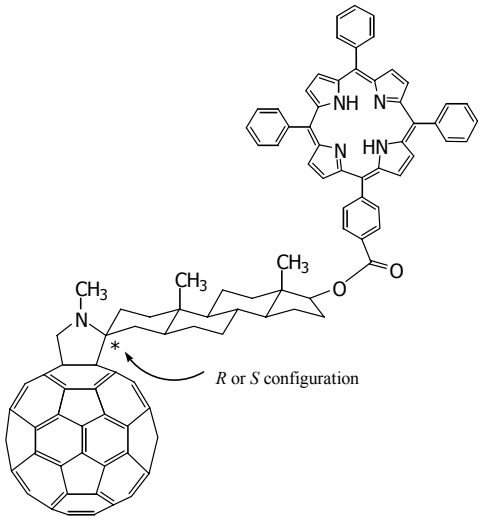

12

It was found that **12** displays biexponential fluorescence decay, with lifetimes of ~ 0.5 and 5 ns. This surprising observation is completely consistent with results of recent computations on the topology of this system [54]. The lowest energy conformation for the *R* diastereomer of **12** was indeed predicted to be the extended one, as originally anticipated, in which the two chromophores are very far apart, with D_{cc} ~ 21.6 Å (see Figure 4b). However, the most stable conformation for the *S* diastereomer is predicted to be the compact structure shown in Figure 4a, in which D_{cc} is only 6.13 Å. To achieve this geometry, the ester linkage is forced to go from *anti* to *syn* in order to bring the P and C_{60} chromophores into close proximity. Thus, PET should be very fast in the *S* diastereomer of **12**, but orders of magnitude slower in the analogous *R* diastereomer, where it is questionable whether PET can even compete with EN. Fullerene triplets could be generated by either pathway. On this basis, it is tempting to assign the observed fluorescence lifetimes of 0.5 and 5 ns to the *S* and *R* diastereomers of **12**, respectively. Hopefully, this can be confirmed by photophysical studies of the separated diastereomers, or at least of samples substantially enriched in one or the other isomer. To our knowledge, dyad **12** would be the first example of a donor-acceptor system in which control of photophysical pathways is directly attributable to a change in configuration at a single carbon atom.

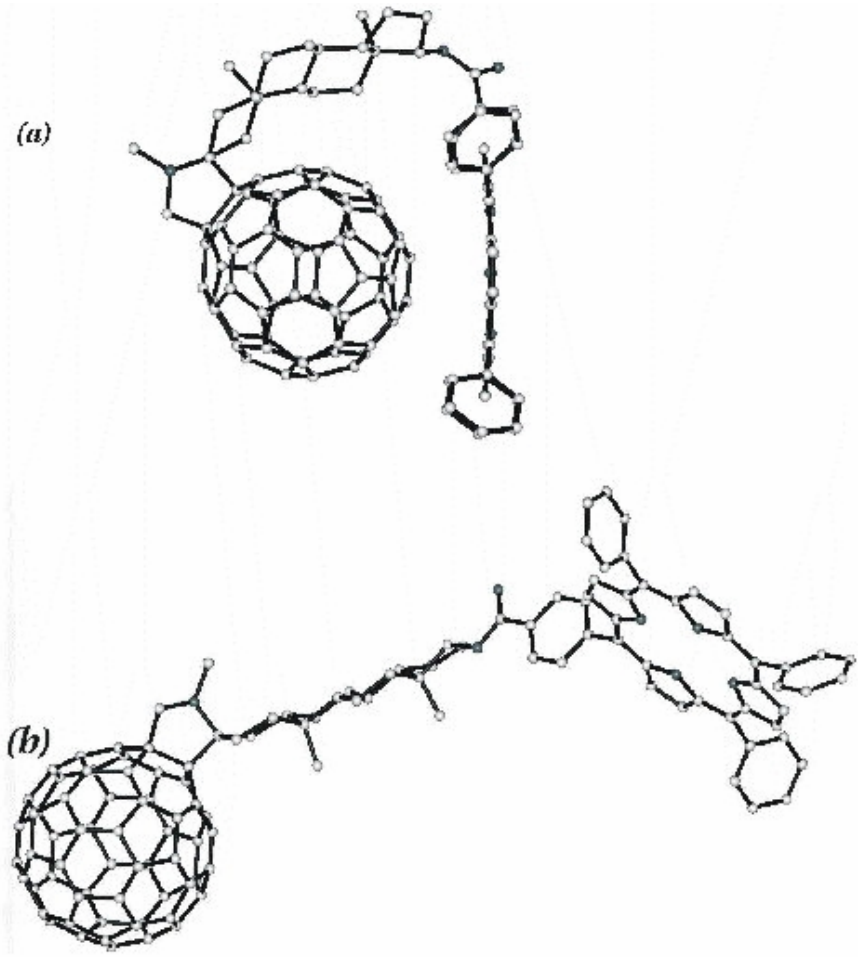

Figure 4. Energy-minimized structures of the *S* diastereomer (a) and the *R* diastereomer (b) of dyad **12**.

4.2.2. *Fullerene-Chlorin Dyads*

There are fewer examples of dyads prepared from fullerenes and chlorins (Ch), close relatives of porphyrins. Rather unexpectedly, the simple zinc chlorin–C_{60} (ZnCh–C_{60}) dyad **13b** exhibited a remarkably long-lived CS state [77]. From CV and spectroscopic studies of the individual moieties, the CS state, $ZnCh^{+\bullet}$–$C_{60}^{\bullet-}$, was determined to lie lower-in-energy than the other pertinent excited states for the system, *i.e.*, $^{1}ZnCh^{*}$–C_{60}, $^{3}ZnCh^{*}$–C_{60}, ZnCh–$^{1}C_{60}^{*}$ and ZnCh–$^{3}C_{60}^{*}$ (see Figure 5b). Following irradiation of **13b** to generate one of the singlet excited states and possibly ISC or EN, ET (k_{ET} = 2.4 x 10^{10} s^{-1}) yielded $ZnCh^{+\bullet}$–$C_{60}^{\bullet-}$. BET gave solely the ground state at a rate of k_{BET} = 9.1 x 10^{3} s^{-1}, as monitored by decay of the transient absorption of $ZnCh^{+\bullet}$ at 790 nm. This rate constant for BET is the slowest of any chlorin or porphyrin-fullerene D–A dyad

studied to date. In the same study, H_2Ch (**13a**) and P–C_{60} (**14**) analogues decayed rapidly to $^3A^*$–D states following BET.

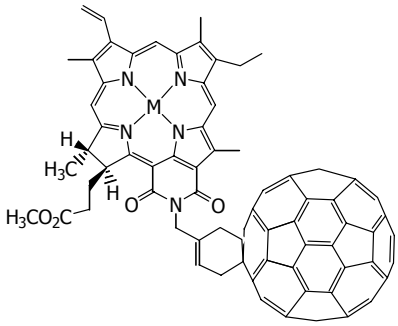

13a M = H_2
13b M = Zn

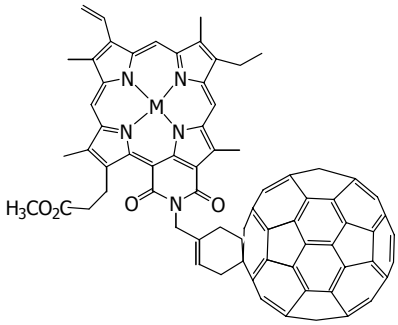

14a M = H_2
14b M = Zn

The small k_{BET} for **13b** was attributed to the small reorganization energy for ET (λ = 0.484 eV), which pushed the event into the Marcus inverted region. It is also important to note the significance of the fact that for **13b** the CS state is the lowest-lying excitation-derived state above the ground state, S_0 (Figure 5b). Thus, in this case, only one BET deactivation process is available. When other excited states lie between the CS and ground states of the dyads, alternative BET processes from the CS state are available (Figure 5a). Since these processes typically have less negative ΔG_{ET} values, BET occurs in the normal or inverse Marcus region at much faster rates, which significantly reduces the lifetime of the CS state.

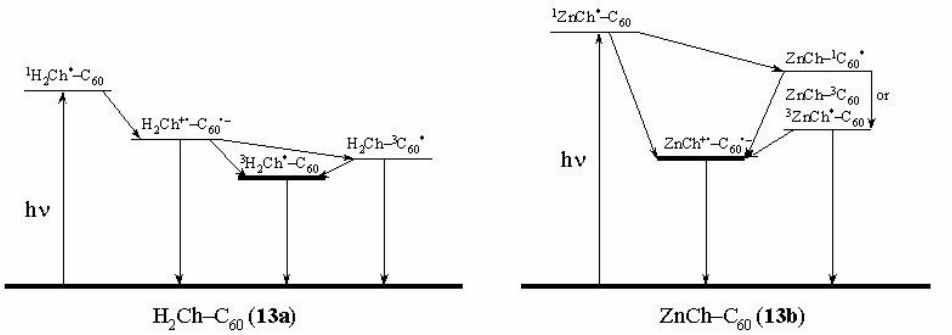

Figure 5. Jablonski diagrams summarizing the photophysical pathways following irradiation of dyads **13a** and **13b**.

Phytochlorin–C_{60} (Pc–C_{60}) dyad **15** exhibited a new excitation energy relaxation pathway: the formation of an intramolecular exciplex [78]. In a non-polar solvent, this exciplex decayed directly to the ground state, whereas in polar solvents it

was a direct precursor to the formation of a full CT state. Although not totally unprecedented [79], exciplex formation in fullerene D–A dyads is rarely observed.

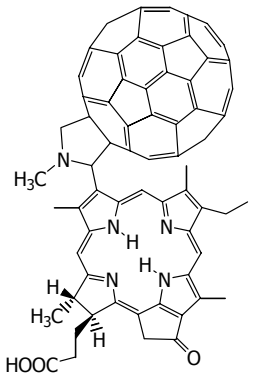

15

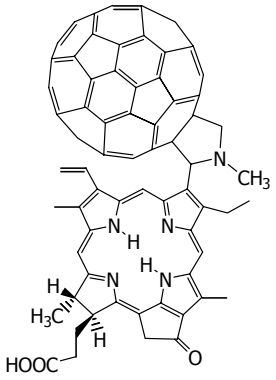

16

A newly synthesized Pc–C_{60} dyad **16** differs from **15** in the position at which the pyrrolidine bridge is linked to the Pc moiety [80]. In **15**, the pyrrolidine bridge is attached to an sp^2 carbon participating in the 18-electron aromatic delocalization pathway of the Pc, whereas in **16** the bridge is attached to an external sp^2 carbon. Upon excitation of the Pc or C_{60} moiety in benzonitrile, both dyads decay to intramolecular exciplexes with characteristic emission bands. Formation of the exciplex also occurs from the second excited singlet state of the phytochlorin, Pc^{2S}–C_{60} → $(Pc–C_{60})^*$, in a process too fast to be resolved with current instruments. However, only dyad **15** is observed by TAS to decay to the ground state *via* a full CT state (τ_{CS} = 65 ps). This result is attributed to the enhanced electronic coupling between the two moieties that is present in **15** but is diminished in **16**.

4.2.3. *Triads Incorporating Fullerene and Porphyrins*

The basic motivation for the synthesis and photophysical investigation of multicomponent molecular arrays incorporating fullerenes is the possibility that such systems might undergo sequential ET steps leading to increased distance between centers of charge and consequently longer lifetimes of CS states (see 2.1.1). The first such system [81] synthesized was the molecular triad **17** in which a diarylporphyrin is linked on one side to a carotenoid polyene and on the other to a fullerene. The triad is symbolized for convenience as C–P–C_{60}. On the basis of ionization potentials, it was anticipated that excitation of either the P or C_{60} moiety would induce ET to give $C–P^{+\bullet}–C_{60}^{\bullet-}$, which would be followed by a second ET step to give $C^{+\bullet}–P–C_{60}^{\bullet-}$. This sequence of events was indeed observed in 2-methyltetrahydrofuran (MTHF), with an overall quantum efficiency of 0.14. The first step is extremely fast, as the lifetimes of C–P–$^1C_{60}^*$ and C–$^1P^*$–C_{60} are only 32 and 10 ps, respectively, from fluorescence decay data. Strong transient absorption at 940 nm confirmed that the product in both cases is $C^{+\bullet}–P–C_{60}^{\bullet-}$, indicating that $C–P^{+\bullet}–C_{60}^{\bullet-}$, which was not detected spectroscopically, evolves very rapidly into the former species by a very rapid second ET step. Similar observations were made in benzonitrile, where the quantum yield for formation of $C^{+\bullet}$–

$P–C_{60}^{\bullet-}$ was 0.12. In toluene, excitation of the porphyrin is followed by singlet-singlet EN to give $C–P–{}^1C_{60}^*$, which then undergoes normal intersystem crossing to give $C–P–{}^3C_{60}^*$; no charge-separated states are detected in this solvent. These findings are consistent with studies of appropriate model systems and dyads discussed earlier.

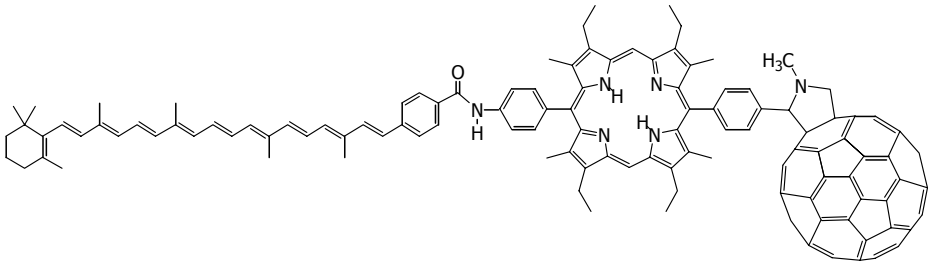

17

However, some extraordinary observations were made with triad **17**. First is the fact that the final CS state decays ($\tau \sim 170$ ns) not to the ground state, but rather to the carotenoid triplet excited state $^3C^*–P–C_{60}$, detected spectroscopically. Even in a MTHF glass at 77 K, excitation of the P moiety of the triad results in formation of $C^{+\bullet}–P–C_{60}^{\bullet-}$ with $\Phi = 0.12$, followed once again by decay to give $^3C^*–P–C_{60}$. This process does not occur upon generation of $C–P–{}^1C_{60}^*$. Thus, ET occurs relatively quickly even at low temperatures, which is very unusual. Most systems studied to date with other types of electron acceptors (including porphyrin-quinone dyads and triads similar to **17** with quinones in place of C_{60}) do not undergo significant photoinduced charge separation in glasses at 77 K [82-84]. Even at 20 K, the formation of $C^{+\bullet}–P–C_{60}^{\bullet-}$ as well as its decay to $^3C^*–P–C_{60}$ could be followed using time resolved electron paramagnetic resonance (EPR) [85]. The rise time of the EPR spectrum of the CS state is too fast to be measured by EPR, even at these very low temperatures, while the rate constant for decay of the carotenoid triplet sublevels at 77 and 20 K are identical and are nearly the same as at 298 K (170 ns). Further mechanistic information comes from the spin polarization in the EPR spectra of the various triplet species. Thus, the polarization pattern for $C–P–{}^3C_{60}^*$, which corresponds to 13% of the total triplet decay at 77 K, indicates it originates by intersystem crossing from the fullerene S_1 state, which is formed to the extent of about 20% upon excitation of **17** at 580 nm. In contrast, the polarization pattern of the $^3C^*–P–C_{60}$, the major triplet component, indicates this species arises by an entirely different route, namely charge recombination from the T_0 level of the triplet radical pair, *i.e.*, $^3[C^{+\bullet}–P–C_{60}^{\bullet-}]$; this species is in equilibrium with the nearly isoenergetic singlet radical pair state, originally formed by ET from $C–{}^1P^*–C_{60}$. Thus, the route to both triplets is completely defined by the experimental data, which is unprecedented.

What is particularly striking is that $C^{+\bullet}–P–C_{60}^{\bullet-}$, which lies 1.24 eV above the S_0 state in polar solvents according to electrochemical data, decays solely to the carotenoid triplet, which is only 0.63 eV above the ground state. The authors argue convincingly that the solvent reorganization energy must be very small at 20 K, and that the internal reorganization energy of C_{60} is expected to be much less than 0.61 eV. In

this case, CR from $C^{+\bullet}$–P–$C_{60}^{\bullet-}$ to give $^3C^*$–P–C_{60} must occur in the Marcus inverted region, and is consequently retarded; however, it is much faster than the even more exergonic process leading to the ground state of the triad. This is in complete contrast to the behavior of a C–P–NQ (NQ = naphthoquinone) triad (**18**), in which the analogous $C^{+\bullet}$–P–$NQ^{\bullet-}$ state (which lies 1.23 eV above the ground state, almost the same as for the fullerene triad) decays at ambient temperatures exclusively to the ground state (S_0) of the triad rather than to the carotene triplet [86]. Moreover, PET for the NQ triad is not observed in a glass at 77 K. These data make it clear that the propensity of the C–P–C_{60} triad to undergo PET even at very low temperatures and the reluctance of the CS state to decay to the ground state, must both be due to the very low reorganization energies associated with electron transfer to and from the fullerene, and cannot be ascribed to excited state energies or differences in oxidation and reduction potentials. This is a dramatic illustration of the special nature of ET in donor-acceptor systems incorporating fullerenes.

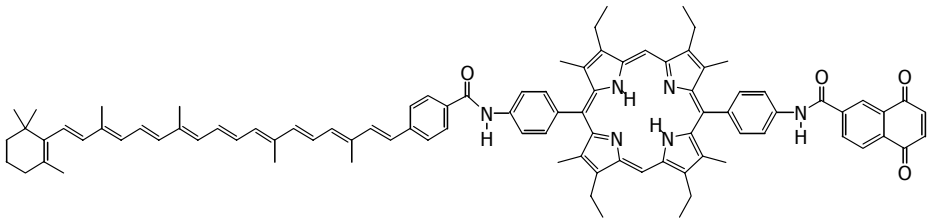

18

A final wrinkle is that the lifetime of the CS state of triad **17** is increased by ~ 50 % in the presence of a small (20 mT) magnetic field at low temperatures [87]. This effect is ascribed to perturbation of the interconversion of the triplet and singlet biradicals by changing the population of the triplet sublevels. The ability of the magnetic field to increase the lifetime of the CS state by slowing charge recombination is potentially applicable in enhancing the utility of such systems in solar energy conversion, and could be the basis of a magnetically controlled optical or optoelectronic switch or logic gate.

By making what would appear to be a relatively minor change in the structure of the C–P–C_{60} triad **17**, namely changing **17** to **17′** by reversing the amide linkage, significant changes in the thermodynamic properties and the photophysics of the triad were observed [88]. Whereas the energies of C–$P^{+\bullet}$–$C_{60}^{\bullet-}$ and $C^{+\bullet}$–P–$C_{60}^{\bullet-}$ are 1.39 and 1.20 eV, respectively, relative to the ground state in the case of **17**, for **17′** the corresponding radical ion pair states have energies of 1.44 and 1.02 eV. While Φ_{CS} for formation of $C^{+\bullet}$–P–$C_{60}^{\bullet-}$ for **17** is ~0.14 in MTHF, the analogous state is formed in the case of **17′** by the same pathway with Φ_{CS} approaching unity over a temperature range from 8 K (rigid glass) to 300 K (fluid solutions). Effects on the lifetime of the CS state are not as dramatic. In MTHF at 292 K, the lifetime of this state increases from 170 ns for **17** up to 340 ns for **17′**, but in benzonitrile the effect is reversed, 770 vs. 470 ns, respectively. In glasses at low temperature, both CS states have lifetimes on the order

of 1 μs. As in the earlier study, the main pathway for decay of $C^{+\bullet}$–P– $C_{60}^{\bullet-}$ in the case of **17′** is formation of $^3C^*$–P–C_{60}, presumably for the reasons discussed above.

It is important to note that the energies of the CS states of the fullerene-based triads and dyads are much less sensitive to changes in dielectric constants of the solvent and to temperature than corresponding quinone-based systems. Thus, production of $C^{+\bullet}$–P–$C_{60}^{\bullet-}$ occurs efficiently at temperatures as low as 8 K [85, 88], whereas PET for corresponding quinone systems begins to drop off at 230 K and is not observable at 77 K, although the energetics are favorable [86]. As already noted, CR from $C^{+\bullet}$–P–$C_{60}^{\bullet-}$ gives the carotene triplet rather than the ground state, while decay of corresponding quinone systems invariably leads to the molecular ground state. Thus, the fullerene-based dyads and triads mimic the behavior of photosynthetic reaction centers much more closely than do the corresponding quinone systems.

Another type of molecular triad involving the covalently-linked array ZnTPP–TPP–C_{60} (see structure **19**) was prepared and studied by Luo *et al.* [89]. The center-to-center distances between the two porphyrins and C_{60} were estimated using CPK modeling as 18.0 and 36.1 Å, respectively. In this system, the ZnTPP serves as the antenna when the triad is excited at 532 nm. In benzonitrile, the initially formed ^{1}ZnTPP*–TPP–C_{60} undergoes singlet-singlet EN with a time constant of 66 ps to generate ZnTPP–^{1}TPP*–C_{60}, which then undergoes ET to give sequentially ZnTPP–TPP$^{+\bullet}$–$C_{60}^{\bullet-}$ and ZnTPP$^{+\bullet}$–TPP–$C_{60}^{\bullet-}$ with time constants of 143 and 465 ps, respectively. The final CS state is formed with an overall quantum yield of 0.4. The most striking observation is that the lifetime of this state is 21 μs in deoxygenated benzonitrile, where decay occurs directly to the ground state ($-\Delta G^{o}_{CR}$ = 1.40 eV). Thus, separation of charge over a longer distance clearly has the effect of increasing the lifetime to the CS state, which is a highly desirable feature of an artificial photosynthetic reaction center complex.

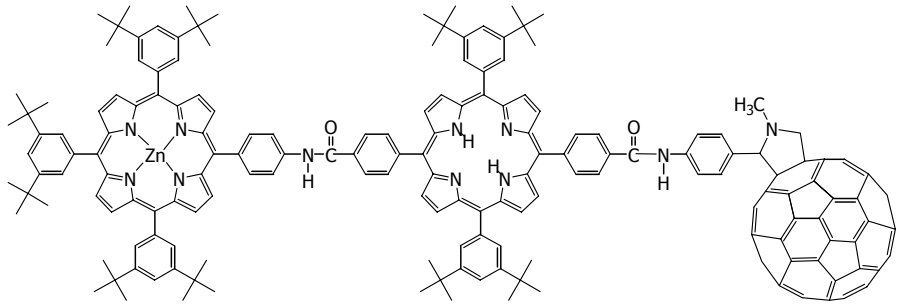

19

Upon photoexcitation of **19** in toluene, ^{1}ZnTPP*–TPP–C_{60} again undergoes singlet-singlet energy transfer to give ZnTPP–^{1}TPP*–C_{60} with a similar time constant of 67 ps, but now energy transfer dominates over ET, generating sequentially ZnTPP–TPP–$^1C_{60}^*$ (87 ps) and then ZnTPP–TPP–$^3C_{60}^*$ (1.8 ns), which then decays by inefficient triplet-triplet energy transfer with a time constant of 4.2 μs to the lowest excited state of the system, ZnTPP–^{3}TPP*–C_{60}. Once again, the marked difference in

the behavior of the system in nonpolar vs. polar solvents is directly attributable to differences in the free energy for charge separation, ΔG^{o}_{CS}, which are -0.29 eV in benzonitrile and + 0.56 eV in toluene, based on electrochemical data.

In accord with expectations based on energy considerations, excitation of the fullerene moiety of **19** at 337 nm in benzonitrile again leads to formation of the CS state with high efficiency, while in toluene energy transfer again dominates. The behavior of the triad is totally in accord with that of the identically substituted dyads, H_2TPP–C_{60} (**20**) and ZnTPP–C_{60} (**21**).

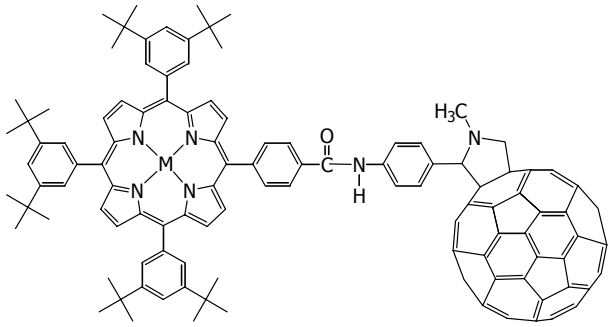

20 M = H_2
21 M = Zn

A systematic study of the photophysics of triad **19**, dyads **20** and **21**, and the analogous ferrocenyl triads Fc–H_2TPP–C_{60} (**22**) and Fc–ZnTPP–C_{60} (**23**), is particularly revealing with respect to the energetics and dynamics of ET processes [51]. The lowest lying CS state of these systems, $Fc^{+\bullet}$–ZnTPP–$C_{60}^{\bullet-}$, is formed with a quantum yield close to unity on excitation of either the ZnTPP or C_{60} moieties, and has a very long lifetime, 16 μs in DMF, 3.7 μs in THF, and 7.7 μs in benzonitrile. The rationalization is that because of the small reorganization energy, forward electron transfer is accelerated and back electron is increased, in the case of both **22** and **23**.

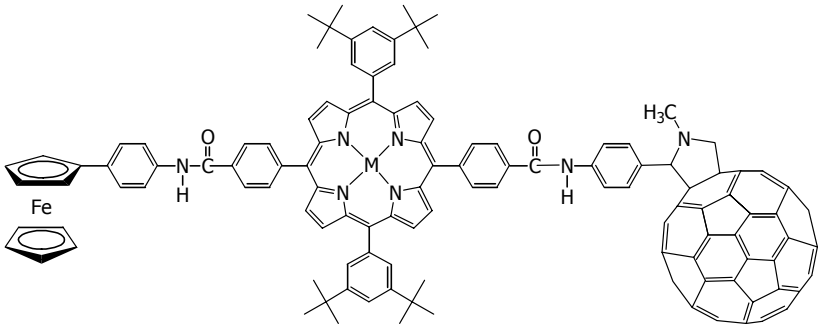

22 M = H_2
23 M = Zn

For both of these systems, k_{CR} decreases with increasing solvent polarity, *i.e.,* lifetimes of CS states are longer in more polar solvents, indicating that CR is in the normal region of the Marcus curve (Figure 2). The opposite trend is observed for the corresponding ZnP systems, namely triad **19** and ZnTPP–C_{60}, indicating that for these systems CR occurs in the inverted region of the Marcus parabola. This is understandable, since the driving force for charge recombination for the Fc systems (0.91 – 1.03 eV) is much smaller than for the ZnTPP systems (1.17 – 1.42 eV). From the best fits to the Marcus equation, the values of the reorganization energy (λ) and the electronic coupling matrix element (V) were determined for all of these systems. The value of λ is considerably larger for the triads than for the dyads, in accord with the difference in donor-acceptor distances, 30.3 vs. 11.9 Å.

4.2.4. *Larger Multicomponent Arrays*

Complexed Porphyrin Arrays. We have already discussed the progress achieved to date in increasing the rate and efficiency of photoinduced ET and simultaneously enhancing the lifetime of CS states by forming covalently-linked multicomponent arrays incorporating fullerenes. An alternative approach is to construct such arrays based on reversible supramolecular interactions between appropriate donor and acceptor moieties. The viability of this new approach is shown by the work of Guldi *et al.*, who found that the electron donor diazabicyclooctane (DABCO) forms 1:1 and 1:2 complexes with the rigid π–π stacked ZnTPP dyad **10**, whose behavior was discussed above [37]. The structures of these complexes, **24** and **25**, respectively, from interaction of DABCO with the central Zn atom in one and two TPP moieties, respectively, are based on firm spectroscopic evidence. The reversible formation of **24** and **25** could be followed by both UV-vis and ^{1}H NMR spectroscopy. Picosecond excitation of both complexes in toluene led to rapid intramolecular ET and transformation of the initially formed ZnTPP S_1 state into a CS radical pair state, exactly as observed in the case of the uncomplexed dyad (see above). However, the lifetimes of the CS states for triad **24** and pentad **25**, 1980 and 2280 ps, respectively, are both markedly enhanced over that of the uncomplexed dyad **10** (619 ps). It is likely that the positive charge in the CS state of **24** and **25** is shared by both the DABCO and ZnTPP moieties.

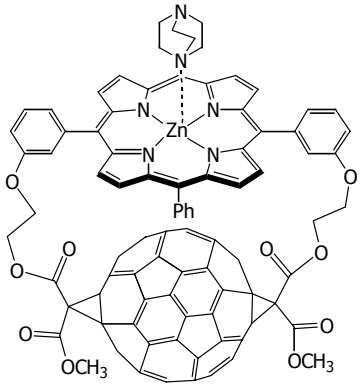

24

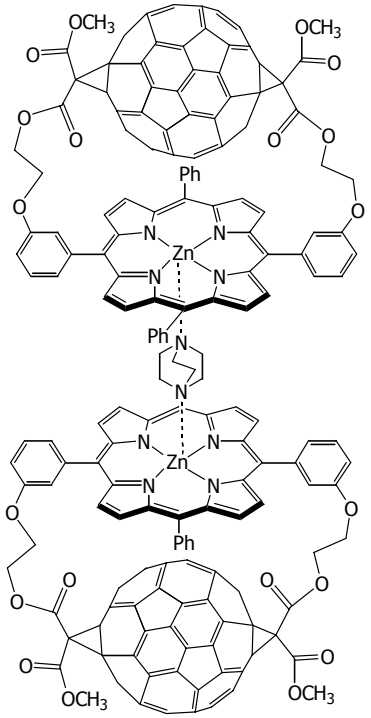

25

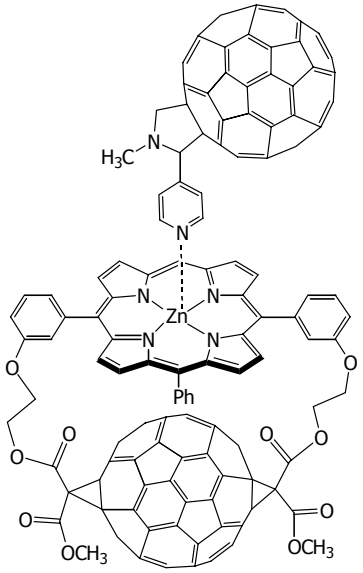

26

An analogous type of complexation was observed between **10** and a fulleropyrrolidine bearing a pyridine group. In **26**, complexation with the pyridine and the Zn did not quench the fluorescence of the ZnTPP moiety in **10**, indicating electron transfer from the porphyrin to the fulleropyridine group, and the reverse, did not take place. While excitation primarily of the P moiety at 532 nm led to no detectable spectral changes, generation of the fullerene S_1 state using 337 nm light activated a two-step process leading eventually to a CS state, *i.e.,* $ZnTPP^{+\bullet}/C_{60}^{\bullet-}$, as shown by the growing in of absorption at 680 nm and 1010 nm, respectively. Both intra- and intermolecular pathways are involved [37].

Artificial Antennas. Another approach to creating more efficient artificial photosynthetic systems is to mimic the natural system by incorporating light-harvesting antennas which absorb visible light and then transfer the excitation to components capable of carrying out chemical reactions, thus converting light energy into chemical energy. In the present context, the objective is to use an artificial antenna to efficiently generate a long-lived charge separated state. An important step in this direction was made by the GMM team, in association with Jon Lindsey at North Carolina State University, by synthesis of a hexad in which three ZnTPP units are linked to a central ZnTPP, which in turn is linked to a free base porphyrin linked to C_{60} (see structure **27**) [90]. As revealed by time-resolved absorption and emission spectroscopy in 2-

methyltetrahydrofuran, selective excitation of any peripheral ZnTPP at 560 nm is followed by singlet-singlet energy transfer to the central ZnTPP to give $(ZnTPP)_3$–$^1ZnTPP^*$–TPP–C_{60} with a time constant of ~ 50 ps. The excitation passes to the free base P with a time constant of 240 ps, generating $(ZnTPP)_3$–ZnTPP–$^1TPP^*$–C_{60}, which decays by ET in 3 ps to give $(ZnTPP)_3$–ZnTPP–$TPP^{+\bullet}$–$C_{60}^{\bullet-}$. This CS state has a lifetime of 1330 ps and is generated with a quantum yield of 0.70.

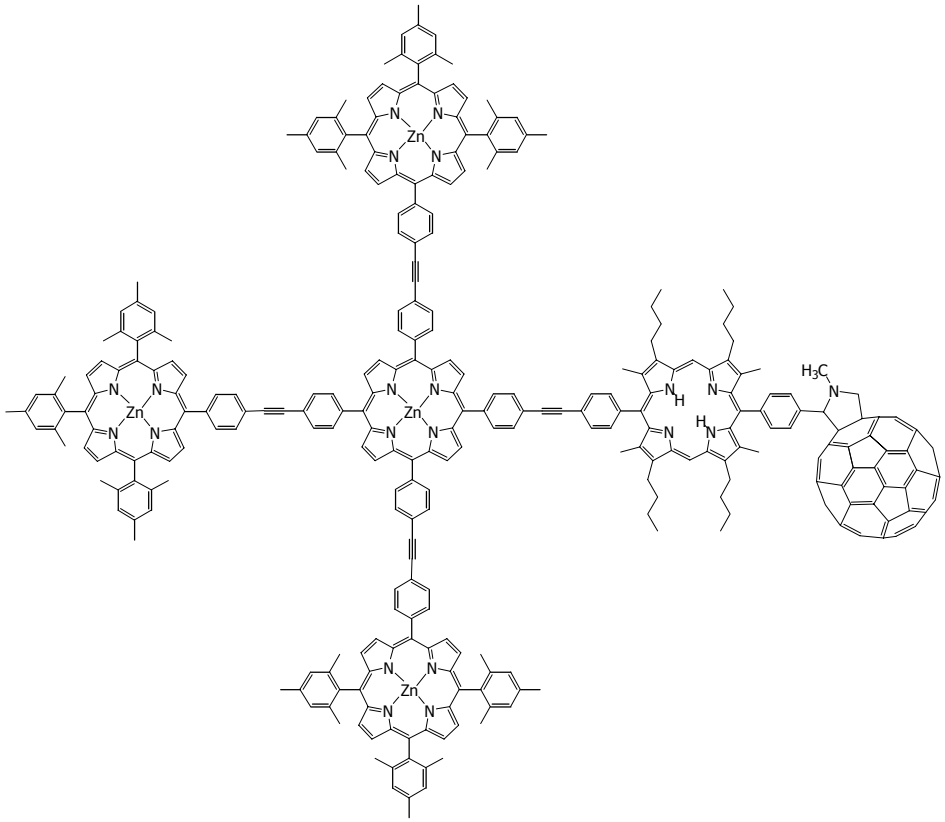

27

Recently, significant progress has been made in this type of system by changing the free base porphyrin to TPP, which affects the energy gradient. In this system [91], the rate of excitation transfer to the free base P is reduced to only 30 ps, and the time constant for electron transfer is 25 ps. Most striking is the observation that the lifetime of the CS state is increased by over two orders of magnitude to 240 ns, and the quantum efficiency for its formation is now 0.9. We await a detailed report on the properties of this hexad.

As pointed out by GMM, even better antenna-reaction center models can be envisaged, incorporating larger light harvesting arrays (possibly based on supramolecular arrays and/or dendrimers), shorter linkers, the use of other metals in place of Zn, and optimal matching of linker connections with electron densities of

frontier molecular orbitals. Despite the enormous synthetic challenges of this type of work, progress along these and probably other lines is anticipated.

4.4. METALLOCENE–C_{60} HYBRIDS

The first study of Fc–C_{60} hybrids showed that ET occurs from the Fc to singlet excited C_{60} [25]. As the lowest singlet excited state of Fc (2.5 eV) lies well above the lowest excited states of monofunctionalized C_{60} (singlet, 1.8 eV; triplet, 1.5 eV), no EN is observed in these systems. A variety of linkers were used to bridge the two moieties. Dyads with saturated bridges had significantly longer lived CS states than those with unsaturated linkers. This suggests BET occurred through bonds in the latter case. Within each series, ET occurred at faster rates as the number of bridging atoms decreased.

Metallocenes, most commonly ferrocene (Fc), have been used in the construction of D–A hybrids owing to their ability to serve as electron donors. The longest lived CS state for a multicomponent array incorporating fullerenes has been reported for tetrad **28**, Fc–ZnTPP–TPP–C_{60}, incorporating sequentially one ferrocene, one ZnTPP, and one free base porphyrin moieties [33]. The thermodynamic driving force for photoinduced charge separation to give $Fc^{+\bullet}$–ZnTPP–TPP–$C_{60}^{\bullet-}$ in benzonitrile is 0.93 eV (compared to 0.70 eV for the triad lacking the Fc group), while the corresponding driving forces for charge recombination (back ET) are 1.11 and 1.34 eV, respectively. The lifetimes of the CS state in frozen media, 380 ms in benzonitrile at 193 K and 340 ms in DMF at 173 K, are by far the longest values yet reported for intramolecular CR in a donor-acceptor ensemble and are comparable with lifetimes of the radical ion pair in bacteria photosynthetic reaction centers [65]. At higher temperatures, lifetimes of the CS state of **28** are markedly reduced due to intermolecular pathways which dominate the dynamics of the decay process.

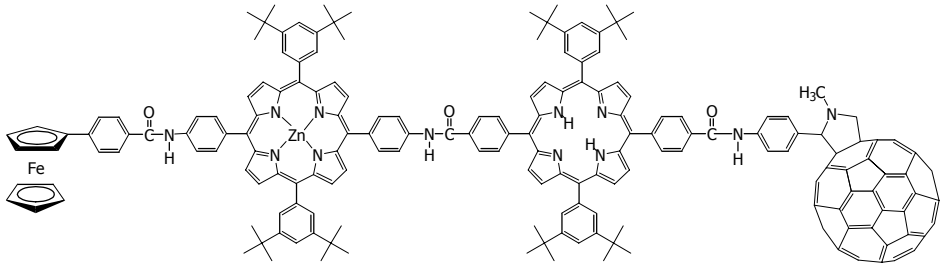

28

Modeled after a hybrid featuring C_{60} functionalized with a Fc-bearing mesomorphic (liquid crystal forming) malonate derivative [92], a novel C_{60} dendrimer featuring eight Fc-containing branches has been prepared [93]. Despite fullerenes being non-mesogenic, the C_{60} moiety appears to have no detrimental effect on the thermal and liquid crystalline properties of the dendrimer. With such D–A fullerodendrimers, researchers hope to create liquid crystalline materials with novel optoelectronic properties [94].

Two ferrocene-porphyrin–C_{60} (Fc–H_2P–C_{60} and Fc–ZnP–C_{60}) triads, **29** and **30**, each appended with an eleven-carbon alkanethiol chain, have been used to create photoactive self-assembled monolayers on Au(111) surfaces [95]. The presence of the easily-oxidized Fc moiety serves to provide an outlet for a charge shift from $P^{+\bullet}$ that distances the oppositely-charged species and leads to longer lived CS states. Upon excitation, the progression of Fc–^{1}ZnP*–C_{60} to Fc–ZnP$^{+\bullet}$–$C_{60}^{\bullet-}$ to Fc$^{+\bullet}$–ZnP–$C_{60}^{\bullet-}$ is observed. An electron is subsequently transferred from the gold electrode to the $Fc^{+\bullet}$, while electron migration from the $C_{60}^{\bullet-}$ to the counter electrode occurs *via* an electron carrier such as $O_2/O_2^{\bullet-}$. The mechanism is probably similar for the Fc–H_2P–C_{60} triad, although the first $^1H_2P^*$–C_{60} ET event might proceed through an exciplex. These systems have a quantum efficiency for photocurrent generation of 20-25%, which are the highest values ever reported for photocurrent generation at monolayer-modified metal electrodes, as well as across artificial membranes, using donor-acceptor linked molecules.

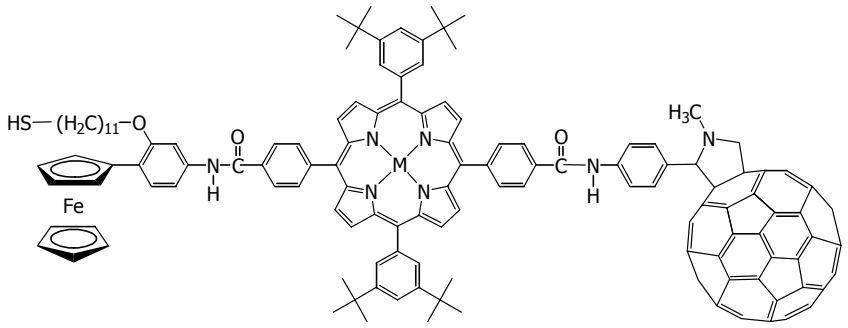

29 M = H_2
30 M = Zn

Subsequent work by Imahori *et al.* in which a mixed SAM was prepared from Fc–H_2P–C_{60} triad **29** and boron-dipyrrin complex **31** produced a SAM with a quantum yield for photocurrent generation of 50 ± 8% and an incident photon-to-current efficiency of 0.6% and 1.6% for irradiation at 510 nm and 430 nm, respectively [96]. The boron-dipyrrin complex enhances the absorption properties in the green and blue regions, and fluorescence lifetime measurements show that the boron-dipyrrin complex photosensitizes the formation of $^1H_2P^*$ following singlet-singlet energy transfer. The efficiencies of these systems are hampered by EN quenching of the singlet excited P moieties by the gold surface.

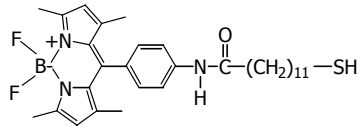

31

4.5. HYBRIDS OF C_{60} WITH RUTHENIUM COMPLEXES

Ruthenium (II) complexes have been shown to act as electron donors *via* metal-to-ligand charge transfer (MLCT) excited states. A number of D–A systems have been prepared and studied in solution and as thin films [1]. Ru(II)–C_{60} dyad **32**, having a rigid androstane linker, exhibited longer-lived CS in polar solvents than the flexibly-linked analogue **33** [75]. Interestingly, BET for the rigid dyad in acetonitrile generates triplet-excited fullerene as opposed to the singlet ground state typically observed. An analogous C_{60}–$[Ru(II)]_2$ dinuclear complex with the same androstane bridge, **34**, was recently prepared, but energy transfer from the MLCT excited state to populate the triplet excited state of C_{60} occurred with only negligible yields of ET [97].

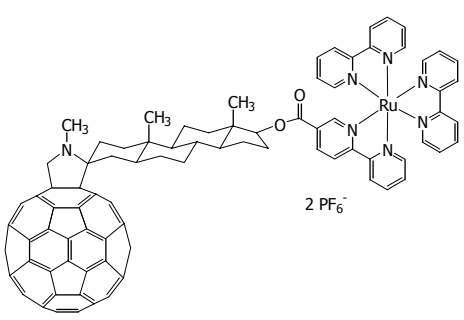

32

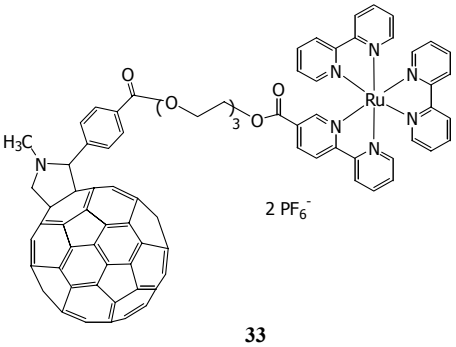

33

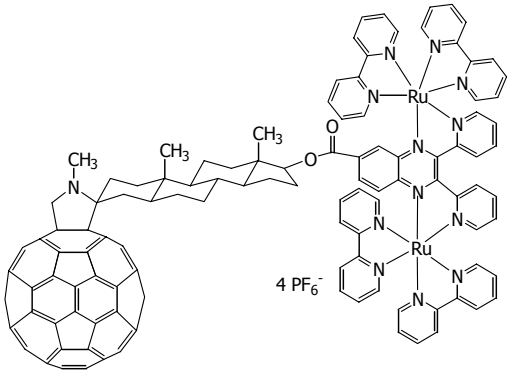

34

A technique for creating better photovoltaic films from covalently-linked fullerene D–A dyads was recently described [98]. The process involved stepwise deposition on a modified semiconductive surface alternatively of a negatively charged organic polysulfonate compound and the positively charged ruthenium (II) dyads **32** and **34** described above. The process is repeated to achieve the desired film thickness, and progress can be monitored by UV absorption. With layers held together by electrostatic forces, the film is remarkably stable and offers distinct advantages over single monolayers of D–A dyads on a gold surface. Following irradiation, the photocurrent

generated at the cathode from the photoexcited fullerene moieties was observed to rise linearly with the number of assembled monolayers. The use of a Ru(II) D–A dyad versus reference fulleropyrrolidines conveniently red-shifts absorption far into the visible spectrum. Attempts at constructing films from Ru complexes without the attached fullerenes were unsuccessful; the hydrophobicity of the cage plays a role in the assembly of the molecules into stable layers.

4.6. CONJUGATED POLYMER AND OLIGOMER HYBRIDS WITH C_{60}

Organic polymers are currently being studied for potential use as organic semiconductors and in photovoltaic cells and devices. The covalent attachment of conjugated polymers to fullerenes, as opposed to nonbonded mixtures of the donors and acceptors, has the distinct advantage of encouraging effective communication as fullerenes often are not soluble in the polymers [99, 100]. For a more detailed discussion of the electron transfer properties of these hybrids in thin films, refer to chapter 14. For their applications as photovoltaic devices, refer to chapter 11.

4.6.1. *Oligophenylenevinylene–C_{60} Hybrids*

In solutions of a series of oligophenylenevinylene–C_{60} hybrids, **35a-c**, EN was observed to occur with no appreciable occurrence of ET [100]. However, when photovoltaic cells were created from these dyads by depositing a thin film on a glass with an indium-tin oxide (ITO) coating, a current was observed upon irradiation. The efficiency of light energy conversion was never greater than 0.03%, which was attributed to the propensity for the competing EN process. Such hybrids offer the advantage that the covalent linkage between D and A creates a bicontinuous network, a circuit that does not have the disadvantage of poor junction contacts, unlike that obtained with noncovalent blends.

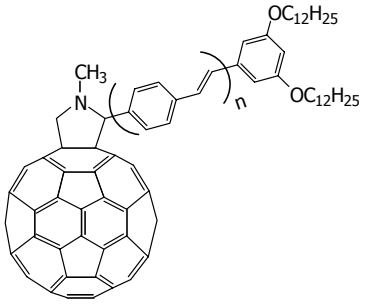

35a n = 0
35b n = 2
35c n = 3

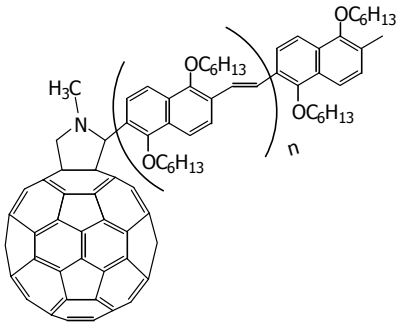

36a n = 0
36b n = 2

In the series of naphthalene oligomer hybrids **36**, however, evidence was presented suggesting that ET competes with dominant singlet-singlet EN, and that the ET pathway increases in prominence with increasing solvent polarity [99]. There were no ground state interactions based on UV and electrochemical studies, but the

fluorescence of the oligomer donors was efficiently quenched while that of C_{60} was observed, indicative of singlet-singlet EN. The decrease in $^3C_{60}^*$ yields as solvent polarity increased suggests ET is a competitive pathway. As confirmation, the triplet absorption spectrum was subtracted from the nanosecond TA spectrum to reveal a maximum at ~1000 nm, indicative of $C_{60}^{\bullet-}$ formed by ET.

Armaroli, Nierengarten and coworkers showed that when an OPV moiety is attached to a fulleropyrollidine, as in **37**, EN prevails over ET even in a relatively polar solvent such as benzonitrile [101]. Thus, spectroscopic fingerprints of the fullerene S_1 and T_1 states (fluorescence and transient triplet absorption at 720 nm, respectively) are observed upon excitation of the fullerene chromophore (at $\lambda > 420$ nm) with unperturbed lifetimes. When the OPV moiety is excited at 365 nm in CH_2Cl_2, the intense OPV fluorescence is quenched with generation of the same fullerene excited states, accompanied by formation of $^1O_2$ with $\Phi = 1.0$, indicating that EN is the exclusive photoinduced process, even in a relatively polar solvent such as benzonitrile, sensitization of fullerene excited states occurs with 70% efficiency, indicating ET competes to a limited extent.

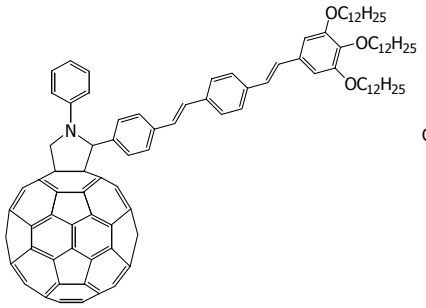

37

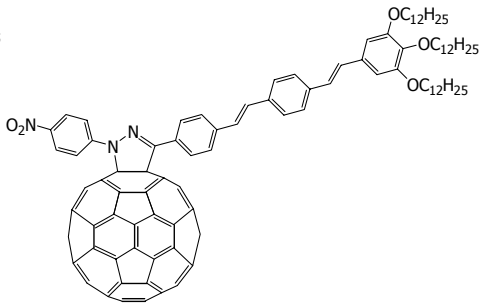

38

The situation changes drastically in the analogous pyrazoline dyad **38** [56]. In CH_2Cl_2,, **38** exhibits quenching of both OPV and C_{60} fluorescence, but no C_{60} triplet absorption or sensitized formation of $^1O_2$ is observed. Furthermore, addition of acid causes recovery of the C_{60} fluorescence. These results demonstrate that both EN (from OPV to C_{60}) and ET (from the nitrogen lone pair in the pyrazoline to electronically excited C_{60}) are in play. At low temperature (77 K in toluene), the latter but not the former process is quenched, consistent with the operation of competitive EN and ET processes. It is apparent that EN from OPV to C_{60} followed by ET can be selectively activated by exciting the OPV moiety, while only ET from the pyrazoline to C_{60} occurs on excitation of the fullerene at longer wavelengths. Moreover, ET can be switched off in this system by addition of acid (*i.e.*, protonation of the pyrazoline) or by lowering the temperature. Thus, by rather minor structural manipulation and variation of reaction conditions, one can selectively activate ET or EN processes, which has strong implications for practical applications of these types of systems.

4.6.2. *Oligothiophene–C_{60} Hybrids*

In solution, intermolecular ET was observed to occur from oligothiophenes (nT, n = 3, 4, 6) and thiophene polymers (poly-T, avg. n ~ 700) to the pristine fullerenes C_{60} and C_{70} (F) [102]. An unsubstituted oligothiophene backbone, **39**, is shown below, although the thiophenes used in this study were appended with six carbon alkyl chains. Following selective excitation of either F or nT, the photodynamics were studied by monitoring the rise and decay of $^3F^*$, $^3nT^*$, $nT^{+\bullet}$, and $F^{\bullet-}$ by flash photoylsis. In a nonpolar solvent (benzene), EN was observed to the exclusion of ET. In polar solvents (benzonitrile, dichlorobenzene) when F was excited, the rate of ET from nT to the $^3F^*$ (k_{ET}) increased as n increased, although the maximum efficiency for ET (Φ_{ET}) occurred with n = 4. EN competed with ET in polar solvents.

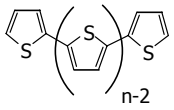

39 nT

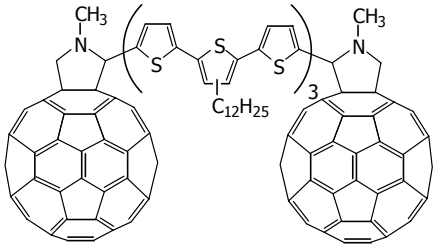

40

When nT was excited in polar solvents, EN prevailed over ET by a ratio of 93:7 for 3T, while for 6T ET occurred with no evidence found for EN. Unlike the case when F was excited, the rate of ET from $^3nT^*$ falls off as n increases, as "negatively larger free-energy changes are expected for shorter oligomers due to their larger triplet energies, which compensate anodic oxidation potentials of shorter oligomers." The poly-T behaved similar to 6T, presumably due to their similar triplet energies and oxidation potentials. BET was observed to occur with second order kinetics, indicative of completely solvated charged intermediates, with rate constants near the diffusion-controlled limits.

A series of C_{60}–nT–C_{60} triads were synthesized and studied in solution, thin films, and in the solid state [103]. In nonpolar solvents, energy transfer from the singlet excited nT moiety to C_{60} was observed followed by near quantitative ISC to $^3C_{60}^*$. In polar solvents, where the energy of the CS state is lowered below that of the excited thiophene, intramolecular ET from $^1nT^*$ to C_{60} was observed. The speed of these events exceeded the resolution of the spectroscopic equipment being used. Subsequent ultrafast femtosecond pump-probe transient absorption studies were required to quantitatively study the very fast photoinduced processes in these systems, and C_{60}–9T–C_{60} triad **40** was chosen for study [104]. Excitation of the thiophene moiety was followed by fast singlet energy transfer (τ = 95 fs) in polar and nonpolar media. In toluene, the fullerene crosses to the triplet state, whereas in the more polar solvent *o*-DCB, a rise in absorption of $9T^{+\bullet}$ is observed throughout the first 30 ps following irradiation. The fact that CT continues long after the 95 fs lifetime of the $^19T^*$ suggests that ET does not occur from $^19T^*$ to C_{60}, but from 9T to $^1C_{60}^*$. The lifetime of $^1C_{60}^*$ is 10 ps, while that of the CS state was 80 ps.

4.7. AMINOFULLERENE HYBRIDS

Amine/C_{60} D–A systems are remarkably versatile, undergoing ET processes intramolecularly as well as intermolecularly, in monomers, clusters, and thin films. The addition of amines to fullerenes is known to occur both thermally and photochemically, with the first step being electron transfer from the amine to $^1C_{60}^*$. These reactions have been reviewed previously [28]; however, a recent study has led to new mechanistic insights. For hydrogenated adducts, the ET step is followed by radical coupling and proton transfer, although the mechanism for formation of dehydrogenated adducts is less clear. In the photochemical addition of triethylamine to C_{60} in the presence of oxygen [105], photoadducts **42** and **43** were formed. While mechanistic data were inconclusive, it was hypothesized that the initially formed product **41**, the only product observed under anaerobic conditions, subsequently underwent further dehydrogenation, intra-, and intermolecular ET processes, to yield the cyclic products **42** and **43**. Fluorescence measurements support this theory. The $^1C_{60}^*$ emission is observed to decrease in increasingly polar solvents, indicative of quenching of the singlet excited C_{60} by ET. The addition of trifluoroacetic acid stopped the quenching process, demonstrating the involvement of the nonbonding electrons on nitrogen in the ET events. Analogous cycloadducts are not observed in the well-studied addition of amines to simple aromatic systems, because the electron accepting ability of the aromatic compound is diminished upon formation of the hydrogenated product. Functionalized fullerenes, however, are still good electron acceptors and potent chromophores.

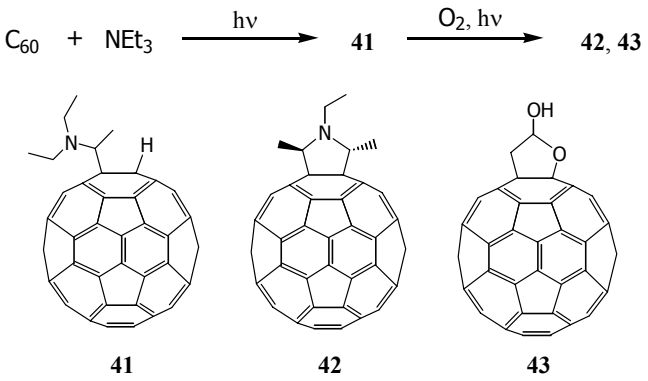

41 **42** **43**

Substituted amines, especially anilines, have been covalently linked to C_{60} and employed as electron donors in various D–A systems. An aniline–C_{60} dyad, **44**, has been synthesized and studied in monomeric form and in clusters [106]. In toluene:acetonitrile solvent systems containing less than 60% acetonitrile, **44** exists in monomeric form. At greater concentrations of acetonitrile, the assembly of **44** into clusters was evident by deviation from the Beer-Lambert law and by a bathochromic shift in UV-vis absorption. For monomeric **44**, BET was observed to occur in faster than 100 ns following irradiation. For a clustered 30 μM sample in 1:3 toluene:acetonitrile, both $^3C_{60}^*$ and $C_{60}^{\bullet-}$ and were observed by TAS with lifetimes of 1.8 μsec and 60 μsec, respectively. The lifetime of the radical anion is dependent upon

the concentration of the dyad, while that of the triplet is not. It was presumed that electron hopping between fullerene cages in the cluster was responsible for retarding BET by separating the charges.

Using varying applied DC voltages, the aniline–C_{60} dyad **44** has been assembled into clusters and deposited on a SnO_2 electrode in thin films of controllable thickness [107]. An electric current is generated upon irradiation of the film due to intramolecular ET followed by electron injection into the SnO_2 electrode from the fullerene radical anion. TAS studies of the film reveal that $C_{60}^{\bullet-}$ can still be detected more than 200 μsec following irradiation, possibly due to the aforementioned intermolecular electron "hopping" throughout the clusters. Photoconversion efficiencies (IPCE) as high as 3-4% at 450 nm were calculated for these systems.

The same researchers prepared a series of aniline–C_{60} dyads (**44-47**) with varying topology [38]. Molecular modeling and ^{1}H NMR studies on these compounds revealed that the preferred conformation for the *ortho* dyads featured the aniline group "folded" onto the cage while in the case of the *para* compounds the aniline donor group was "extended" away from the cage. In toluene, the fluorescence quantum yields and lifetimes of $^1C_{60}^*$ for all four compounds mirrored a model fulleropyrrolidine. In benzonitrile, however, the singlet lifetimes shortened significantly. Rates for charge separation were calculated based on fluorescence quenching relative to the reference compound. The results are summarized in Table 3. The faster rates for ET and higher quantum yields of the CS state for the *ortho* dyads *vis à vis* the *para* dyads are attributed to the closer orientation of the aniline donor moieties to the C_{60} cage. In the *para* isomers, ISC to the triplet state competes more favorably. Transient absorption of the C_{60} radical anion was observed for **45** and **47**, but could not be detected for **44** and **46**. This is indicative of BET events occurring faster in the latter pair, in which there are shorter linkages between the D and A moieties.

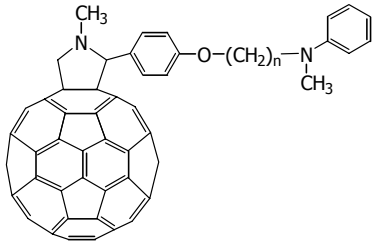

44 n = 2
45 n = 3

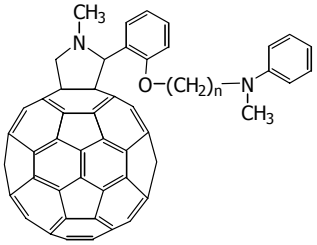

46 n = 2
47 n = 3

TABLE 3. Photophysical data for dyads **44**-**47**, a series of aminofullerenes with various linkage topologies.

	Toluene			**Benzonitrile**				
Dyad	τ_S (ns)	τ_T (μs)	Φ_T	τ_S (ns)	τ_T (μs)	k_{CS} ($10^9 s^{-1}$)	Φ_{CS}	Φ_T
44	1.27	16.2	0.92	0.90	8.5	0.35	0.32	0.67
45	1.20	13.2	0.95	0.70	7.4	0.67	0.47	0.49
46	1.25	13.4	0.95	< 0.30	2.2	> 2.5	> 0.77	0.18
47	1.14	14.4	0.95	< 0.30	6.6	> 2.5	> 0.77	0.15

4.8. OXIDATION OF C_{60}

Although oxidation of C_{60} is considerably more difficult than reduction, the generation of $C_{60}^{+\bullet}$ has been achieved by a number of methods, recently reviewed by Reed and Bolskar [108]. Electrochemical oxidation of C_{60} was observed to occur in benzonitrile at a potential of +1.76 V vs. SCE [109]. The photochemical generation of $C_{60}^{+\bullet}$ was achieved by γ-irradiation of C_{60} in a glass at 77 K, and TAS could be used to monitor its production by its absorption maximum at 980 nm [110]. Foote and coworkers generated $C_{60}^{+\bullet}$ *via* photoinduced electron transfer to singlet-excited N-methylacridinium hexaflurophosphate ($^1MA^+$, E_{red} = +2.31 V) [111]. The quantum yield for this process was improved by introduction of biphenyl (BP) as a cosensitizer, where $^1MA^+$ first oxidized BP to form BP^+ (E_{red} = 1.96 V), which has a longer lifetime than $^1MA^+$; BP^+ in turn oxidizes C_{60} to form $C_{60}^{+\bullet}$. The photoxidizing agent 9,10-dicyanoanthracene (DCA) has also been employed to generate $C_{60}^{+\bullet}$, which was subsequently trapped by methanol to generate hydromethoxy adducts, or hydroalkylated adducts in the absence of nucleophilic solvent [112]. Reed *et al*. have produced $C_{60}^{+\bullet}$ by electron transfer to hexabromophenyl-carbazole$^{+\bullet}$/$CB_{11}H_6X_6^-$) in solution [113]. More recently, Fukuzumi and coworkers reported that scandium(III) triflate promotes electron transfer from $^3C_{60}^*$ to *p*-chloranil and *p*-benzoquinone in benzonitrile [114]. Under identical conditions, no ET was observed to occur in the absence of the Sc^{3+} ion.

5. Conclusions

5.1. CURRENT DIRECTIONS IN RESEARCH

A great deal of progress has been made in understanding how D–A systems can be improved in hopes of eventually creating systems of commercial or practical value. The main goal of many of these projects has been to mimic the process of photosynthesis by the conversion of light into electrical or chemical energy. While the success of photosynthesis can be monitored by the production of ATP or NADPH, quantitative assessments of the artificial systems are less precise. The quantum yield (Φ_{CS}) and lifetime (τ_{CS}) of the charge-separated state following ET are measures of achievement in artificial photosynthesis systems. The working assumption is that the slower the rate of BET, the greater the chance that a subsequent process can convert the potential energy of the CS state into some "usable" form of energy. Operating on this assumption, there are three primary strategies that have proven successful in lengthening the lifetime of the CS state by retarding BET.

5.1.1. *Pushing Back ET into the Marcus Inverted Region by Decreasing the Reorganization Energy.*
Marcus electron transfer theory predicts that past a certain point, the rate of an electron transfer process (k_{ET}) is slowed by an increase in the thermodynamic driving force ($-\Delta G_{ET}$) by the process [13-15]. Events in this "inverted region" occur when $-\Delta G_{ET} > \lambda$, where λ is the reorganization energy associated with the compound and solvent molecules following electron transfer (see Figure 2). While the increased use of C_{60} as

an electron acceptor could be attributed, in part, to an increased availability of this exotic organic material, its sustained use can be ascribed to the low reorganization energy associated with ET due to its three-dimensional symmetry. One experimental approach is to construct dyads with the aim of further lowering reorganization energy following ET events, especially for back electron transfer to the ground state. In constructing systems with lower reorganization energies, there will be greater chances of finding events that satisfy $-\Delta G_{ET} > \lambda$, taking advantage of the Marcus inverted region to slow energy-wasting BET processes selectively. It appears that λ is smallest within compact rigid hybrids in which D and A are in close proximity and in which the solvent is excluded from the region between the two moieties.

5.1.2. *Finding Photoinduced Electron Donors With High Triplet Energies and Low Oxidation Potentials.* The work of Fukazumi *et al*. [77] has unequivocally demonstrated the importance of ensuring that the CT state ($D^{+\bullet}$–B–$A^{\bullet-}$) is the lowest excited state of hybrid systems. Otherwise, fast BET relaxation processes to generate lower energy excited states, *e.g.*, D–B–$^3A^*$ or $^3D^*$–B–A, will reduce or erase the prospect of harvesting the potential energy of the system. The key is to find electron donating chromophores with low oxidation potentials and relatively high-lying triplet states. In this respect, chlorins appear to be superior photoinducable electron donors relative to porphyrins, and even better species will undoubtedly be identified in the near future.

5.1.3. *Increasing Charge Separation in Multicomponent Hybrids Using Electron Transfer Cascades.* A number of systems have demonstrated the success of linking a series of electroactive moieties to C_{60} to form a redox gradient, where multiple ET events act to separate the ejected electron from the donor chromophore. As the rate of ET varies with the inverse of distance to the sixth power, increasing spatial separation has a profound impact on retarding the possibility of energy-wasting BET. This effect has been proven in triads, tetrads, and supramolecular clusters containing fullerenes.

5.1.4. *Demonstrated and Potential Biological Applications.* One of the key goals in studies of photoinduced electron transfer is to create systems which can mimic photosynthetic energy transduction, by activating processes of biological significance. Some of the key ideas and approaches are clearly summarized in a recent article by GMM [16]. Thus, just as light-activated bacterial photosynthetic reaction centers are able to drive proton transfer across lipid bilayers and ultimately induce the transformation of ADP into ATP, an important objective is to see if artificial reaction centers incorporated into bilayers containing all the necessary machinery (*i.e.*, cytochrome *c*, ATP synthase, quinone, *etc.*) can accomplish the same thing. The problem here is find systems in which (a) high energy long-lived charge separated states can be generated, and (b) which can be incorporated directionally into properly constituted lipid bilayers so that protons can be pumped from one side of the membrane to the other. This has been accomplished using a carotene-porphyrin-quinone triad **48** [115]. The hydrophobic carotenoid moiety enters the hydrophobic core of the membrane while the negatively-charged carboxylate group is near the hydrophilic exterior. This anchors the systems so it points in one direction, and on excitation acts as

a light-driven proton pump. It was shown that the proton motive force generated by this artificial system indeed was capable of driving ATP synthesis.

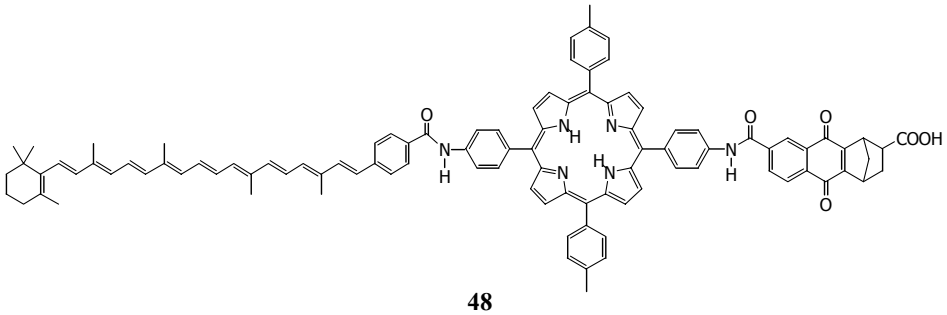

48

To date, no artificial system incorporating fullerenes has been reported which is able to accomplish the same objectives. The problem here is to synthesize molecular arrays analogous to **48** which can be unidirectionally inserted into liposome vesicles, that is, which have clearly definable hydrophobic and hydrophilic ends. In order to differentiate the hydrophobic fullerene residue from the hydrophobic carotenoid and/or porphyrin residues at the other end, one would have to incorporate hydrophilic residues onto the fullerene moiety in the otherwise promising hybrids discussed above. This problem in molecular engineering has yet to be solved.

However, Fukuzumi *et al.* recently succeeded at mimicking a different biochemical process [116]. The system NADH/NAD^+ (NAD^+ = nicotinamide adenine dinucleotide) plays a key role in biological redox systems in energy conversion and storage. It was recently reported that CS states generated photochemically from triad **19** and dyad **20** react with NADH analogues in the presence of hexyl viologen (HV^{2+}) in an extremely efficient process, in which the $ZnTPP^{+\bullet}$ undergoes one electron reduction and $C_{60}^{\bullet-}$ is simultaneously oxidized. Thus, the triad and dyad are efficient photocatalysts of the uphill oxidation of NADH analogues, with a quantum yield equal to that for generation of the CS states, as discussed above.

5.2. CONCLUSIONS AND OUTLOOK

The sustained volume and quality of research involving the construction and exploitation of functionalized fullerene hybrids is a testament to the importance of the field. Great accomplishments have been made in the past two years in the synthesis of hybrids with novel topologies, in the goal of increasing charge-separated state lifetime, and in developing new experimental methods for studies of their photophysical behavior. The prospect for finding practical applications for functionalized fullerenes continues to grow with the field.

5.3. ACKNOWLEDGMENTS

The completion of this chapter would not have been possible without the imagination and experimental skill of the colleagues whose work appears in the references. The authors gratefully acknowledge all of those who have contributed ideas and experimental data to this field. We wish to thank the National Science Foundation for funding the research in this area conducted at NYU. P.J.B. wishes to extend his appreciation to the NYU College of Arts and Science for the Morse Scholarship that has supported his undergraduate education and research, as well as the Arnold and Mabel Beckman Foundation Scholars Program for additional research support.

6. References

1. Guldi, D.M. and Kamat, P.V. (2000) in *Fullerenes: Chemistry, Physics, and Technology,* ed. R. S. Ruoff, John Wiley & Sons, Inc., New York p. 225-281
2. Martín, N., Sánchez, L., Illescas, B. and Pérez, I. (1998) C_{60}-Based Electroactive Organofullerenes, *Chem. Rev.* **98**, 2527-2547.
3. Guldi, D.M. and Prato, M. (2000) Excited-State Properties of C_{60} Fullerene Derivatives, *Acc. Chem. Res.* **33**, 695-703.
4. Guldi, D.M. (2000) Fullerenes: Three Dimensional Electron Acceptor Materials, *Chem. Commun.*, 321-327.
5. Imahori, H. and Sakata, Y. (1999) Fullerenes as Novel Acceptors in Photosynthetic Electron Transfer, *Eur. J. Org. Chem.*, 2445-2457.
6. Kroto, H.W., Heath, J.R., O'Brien, S.C., Curl, R.F. and Smalley, R.E. (1985) C_{60}: Buckminsterfullerene, *Nature* **318**, 162-163.
7. Echegoyen, L., Diederich, F. and Echegoyen, L.E. (2000) in *Fullerenes: Chemistry, Physics, and Technology,* ed. R. S. Ruoff, John Wiley & Sons, Inc., New York p. 1-51
8. Jensen, A.W., Wilson, S.R. and Schuster, D.I. (1996) Biological Applications of Fullerenes, *Biorg. Med. Chem.* **4**, 767-779.
9. Wilson, S.R. (2000) in *Fullerenes: Chemistry, Physics, and Technology,* ed. R. S. Ruoff, John Wiley & Sons, Inc., New York p. 437-465
10. Ros, T.D. and Prato, M. (1999) Medicinal Chemistry with Fullerenes and Fullerene Derivatives, *Chem. Commun.*, 663-669.
11. Imahori, H., El-Khouly, M.E., Fujitsuka, M., Ito, O., Sakata, Y. and Fukuzumi, S. (2001) Solvent Dependence of Charge Separation and Charge Recombination Rates in Porphyrin-Fullerene Dyad, *J. Phys. Chem. A* **105**, 325-332.
12. Schuster, D.I., Cheng, P., Wilson, S.R., Prokhorenko, V., Katterle, M., Holzwarth, A.R., Braslavsky, S.E., Klihm, G., Williams, R.M. and Luo, C. (1999) Photodynamics of a Constrained Parachute-Shaped Fullerene-Porphyrin Dyad, *J. Am. Chem. Soc.* **121**, 11599-11600.
13. Marcus, R.A. (1964) Chemical and Electrochemical Electron-Transfer Theory, *Ann. Rev. Phys. Chem.* **15**, 155-196.
14. Marcus, R.A. and Sutin, N. (1985) Electron Transfers in Chemistry and Biology, *Biochim. Biophys. Acta* **811**, 265-322.
15. Marcus, R.A. (1993) Electron-Transfer Reactions in Chemistry: Theory and Experiment, *Angew. Chem. Int. Ed. Engl.* **32**, 1111-1121.
16. Gust, D., Moore, T.A. and Moore, A.L. (2001) Mimicking Photosynthetic Solar Energy Transduction, *Acc. Chem. Res.* **34**, 40-48.
17. Imahori, H. and Sakata, Y. (1997) Donor-Linked Fullerenes: Photoinduced Electron Transfer and Its Potential Application, *Adv. Mater.* **9**, 537-546.
18. Arbogast, J.W., Darmanyan, A.P., Foote, C.S., Rubin, Y., Diederich, F.N., Alvarez, M.M., Anz, S.J. and Whetten, R.L. (1991) Photophysical Properties of C_{60}, *J. Phys. Chem.* **95**, 11-12.
19. Ebbesen, T.W., Tanigaki, K. and Kuroshima, S. (1991) Excited-State Properties of C_{60}, *Chem. Phys. Lett.* **181**, 501-504.

20. Mattay, J., Ulmer, L. and Sotzmann, A. (2001) in *Understanding and Manipulating Excited-State Processes,* ed. K. S. Schanze, Marcel Dekker, Inc., New York 637-752
21. Khan, A.U. and Kasha, M. (1979) Direct Spectroscopic Observation of Singlet Oxygen Emission at 1268 nm Excited by Sensitizing Dyes of Biological Interest in Liquid Solution, *Proc. Natl. Acad. Sci. USA* **76**, 6047-6049.
22. Fraelich, M.R. and Weisman, R.B. (1993) Triplet States of C_{60} and C_{70} in Solution: Long Intrinsic Lifetimes and Energy Pooling, *J. Phys. Chem.* **97**, 11145-11147.
23. Sun, Y.-P., Wang, P. and Hamilton, N.B. (1993) Fluorescence Spectra and Quantum Yields of Buckminsterfullerene (C_{60}) in Room-Temperature Solutions. No Excitation Wavelength Dependence, *J. Am. Chem. Soc.* **115**, 6378-6381.
24. Zeng, Y., Biczok, L. and Linschitz, H. (1992) External Heavy Atom Induced Phosphorescence Emission of Fullerenes: The Energy of Triplet C_{60}, *J. Phys. Chem.* **96**, 5237-5239.
25. Guldi, D.M., Maggini, M., Scorrano, G. and Prato, M. (1997) Intramolecular Electron Transfer in Fullerene/Ferrocene Based Donor-Bridge-Acceptor Dyads, *J. Am. Chem. Soc.* **119**, 974-980.
26. Krätschmer, W., Lamb, L.D., Fostiropoulos, K. and Huffman, D. (1990) Solid C_{60}: A New Form of Carbon, *Nature* **347**, 354-358.
27. Wilson, S.R., Schuster, D.I., Nuber, B., Meier, M.S., Maggini, M., Prato, M. and Taylor, R. (2000) in *Fullerenes: Chemistry, Physics, and Technology,* ed. R. S. Ruoff, John Wiley & Sons, Inc., New York p. 91-176
28. Hirsch, A. (1994) *The Chemistry of the Fullerenes,* Thieme, Stuttgart.
29. Diederich, F. and Kessinger, R. (1999) Templated Regioselective and Stereoselective Synthesis in Fullerene Chemistry, *Acc. Chem. Res.* **32**, 537-545.
30. Hall, D.O. and Rao, K.K. (1999) *Photosynthesis,* Cambridge University Press, Cambridge, England.
31. Jordan, P., Fromme, P., Witt, H.T., Klukas, O., Saenger, W. and Krauß, N. (2001) Three-Dimensional Structure of Cyanobacterial Photosystem I at 2.5 Å Resolution, *Nature* **411**, 909-917.
32. Iwaki, M., Kumazaki, S., Yoshihara, K., Erabi, T. and Itoh, S. (1996) ΔG^0 Dependence of the Electron Transfer Rate in the Photosynthetic Reaction Center of Plant Photosystem I: Natural Optimization of Reaction between Chlorophyll *a* (A_0) and Quinone, *J. Phys. Chem.* **100**, 10802-10809.
33. Imahori, H., Guldi, D.M., Tamaki, K., Yoshida, Y., Luo, C., Sakata, Y. and Fukuzumi, S. (2001) Charge Separation in a Novel Artificial Photosynthetic Reaction Center Lives 380 ms, *J. Am. Chem. Soc.* **123**, 6617-6628.
34. Gust, D., Moore, T.A., Moore, A.L., Kuciauskas, D., Liddell, P.A. and Halbert, B.D. (1998) Mimicry of Carotenoid Photoprotection in Artificial Photosynthetic Reaction Centers: Triplet-Triplet Energy Transfer by a Relay Mechanism, *Photochem. Photobiol. B* **43**, 209-216.
35. Imahori, H., Tkachenko, N.V., Vehmanen, V., Tamaki, K., Lemmetyinen, H., Sakata, Y. and Fukuzumi, S. (2001) An Extremely Small Reorganization Energy of Electron Transfer in Porphyrin-Fullerene Dyad, *J. Phys. Chem. A* **105**, 1750-1756.
36. MacMahon, S.A. and Schuster, D.I. (2001), Unpublished results.
37. Guldi, D.M., Luo, C., Ros, T.D., Prato, M., Dietel, E. and Hirsch, A. (2000) Photoinduced Electron Transfer in Multicomponent Arrays of a Pi-Stacked Fullerene Porphyrin Dyad and Diazabicyclooctane or a Fulleropyrrolidine Ligand, *Chem. Commun.*, 375-376.
38. Thomas, K.G., Biju, V., Guldi, D.M., Kamat, P.V. and George, M.V. (1999) Orientation-Dependent Electron Transfer Processes in Fullerene-Aniline Dyads, *J. Phys. Chem. A* **103**, 10755-10763.
39. Boyd, P.D.W., Hodgson, M.C., Rickard, C.E.F., Oliver, A.G., Chaker, L., Brothers, P.J., Bolskar, R.D., Tham, F.S. and Reed, C.A. (1999) Selective Supramolecular Porphyrin/Fullerene Interactions, **121**, 10487-10495.
40. Liddell, P.A., Sumida, J.P., Macpherson, A.N., Noss, L., Seely, G.R., Clark, K.N., Moore, A.L., Moore, T.A. and Gust, D. (1994) Preparation and Photophysical Studies of Porphyrin-C_{60} Dyads, *Photochem. Photobio.* **60**, 537-541.
41. Saunders, M., Jimenez-Vazquez, H.A., Cross, R.J., Mroczkowski, S., Gross, M.L., Giblin, D.E. and Poreda, R.J. (1994) Incorporation of Helium, Neon, Argon, Krypton, and Xenon into Fullerenes Using High Pressure, *J. Am. Chem. Soc.* **116**, 2193-2194.
42. Saunders, M., Jimenez-Vazquez, H.A., Cross, R.J., Mroczkowski, S., Freedberg, D.I. and Anet, F.A.L. (1994) Probing the Interior of Fullerenes by ^{3}He NMR Spectroscopy of Endohedral $^3He@C_{60}$ and $^3He@C_{70}$, *Nature* **367**, 256-258.

43. Saunders, M., Jimenez-Vazquez, H.A., Bangerter, B.W., Cross, R.J., Mroczkowski, S., Freedberg, D.I. and Anet, F.A.L. (1994) ^{3}He NMR: A Powerful New Tool for Following Fullerene Chemistry, *J. Am. Chem. Soc.* **116**, 3621-3622.
44. Saunders, M., Cross, R.J., Jimenez-Vazquez, H.A., Shimshi, R. and Khong, A. (1996) Noble Gas Atoms Inside Fullerenes, *Science* **271**, 1693-1697.
45. Cheng, P., Wilson, S.R. and Schuster, D.I. (1999) A Novel Parachute-Shaped C_{60}-Porphyrin Dyad, *Chem. Commun.*, 89-90.
46. Kuciauskas, D., Lin, S., Seely, G.R., Moore, A.L., Moore, T.A., Gust, D., Drovetskaya, T., Reed, C.A. and Boyd, P.D.W. (1996) Energy and Photoinduced Electron Transfer in Porphyrin-Fullerene Dyads, *J. Phys. Chem.* **100**, 15926-15932.
47. Anderson, J.L., An, Y.-Z., Rubin, Y. and Foote, C.S. (1994) Photophysical Characterization and Singlet Oxygen Yield of a Dihydrofullerene, *J. Am. Chem. Soc.* **116**, 9763-9764.
48. Bensasson, R.V., Bienvenue, E., Janot, J.-M., Leach, S., Seta, P., Schuster, D.I., Wilson, S.R. and Zhao, H. (1995) Photophysical Properties of Three Hydrofullerenes, *Chem. Phys. Lett.* **245**, 566-570.
49. Guldi, D.M. and Asmus, K.-D. (1997) Photophysical Properties of Mono- and Multiply-Functionalized Fullerene Derivatives, *J. Phys. Chem. A* **101**, 1472-1481.
50. Echegoyen, L. and Echegoyen, L.E. (1998) Electrochemistry of Fullerenes and Their Derivatives, *Acc. Chem. Res.* **31**, 593-601.
51. Imahori, H., Tamaki, K., Guldi, D.M., Luo, C., Fujitsuka, M., Ito, O., Sakata, Y. and Fukuzumi, S. (2001) Modulating Charge Separation and Charge Recombination Dynamics in Porphyrin-Fullerene Linked Dyads and Triads: Marcus-Normal versus Inverted Region, *J. Am. Chem. Soc.* **123**, 2607-2617.
52. Gilbert, A. and Baggott, J. (1991) *Essentials of Molecular Photochemistry,* Blackwell Scientific, Oxford.
53. Macdonald, I.J. and Dougherty, T.J. (2001) Basic Principles of Photodynamic Therapy, *J. Porphyrins Phthalocyanines* **5**, 105-129.
54. Schuster, D.I., Jarowski, P.D., Kirschner, A.N. and Wilson, S.R. (2001) Molecular Modeling of Porphyrin-Fullerene Dyads, submitted for publication.
55. Guldi, D.M., Luo, C., Prato, M., Troisi, A., Zerbetto, F., Scheloske, M., Dietel, E., Bauer, W. and Hirsch, A. (2001) Parallel (Face-to-Face) Versus Perpendicular (Edge-to-Face) Alignment of Electron Donors and Acceptors in Fullerene Porphyrin Dyads: The Importance of Orientation in Electron Transfer, *J. Am. Chem. Soc.* **123**, 9166-9167.
56. Nierengarten, J.-F., Private communication of unpublished results.
57. Beeby, A., Eastoe, J. and Crooks, E.R. (1996) Remarkable Stability of C_{60}^{-} in Micelles, *Chem. Commun.*, 901-902.
58. Guldi, D.M. (1997) Electron Transfer Studies in C_{78} (C_{2v}'), C_{76} (D_2), C_{70} (D_{5h}), and C_{60} (I_h) Surfactant Aqueous Solutions, *J. Phys. Chem. B* **101**, 9600-9605.
59. Olmstead, M.M., Costa, D.A., Maitra, K., Noll, B.C., Phillips, S.L., Calcar, P.M.V. and Balch, A.L. (1999) Interaction of Curved and Flat Molecular Surfaces. The Structures of Crystalline Compounds Composed of Fullerene (C_{60}, $C_{60}O$, C_{70}, and $C_{120}O$) and Metal Octaethylporphyrin Units, *J. Am. Chem. Soc.* **121**, 7090-7097.
60. Balch, A.L. and Olmstead, M.M. (1998) Reactions of Transition Metal Complexes with Fullerenes (C_{60}, C_{70}, *etc.*) and Related Materials, *Chem. Rev.* **98**, 2123-2165.
61. Eichhorn, D.M., Yang, S., Jarrell, W., Baumann, T.F., Beall, L.S., White, A.J.P., Williams, D.J., Barrett, A.G.M. and Hoffman, B.M. (1995) [60]Fullerene and TCNQ Donor-Acceptor Crystals of Octakis(dimethylamino)porphyrazine, *Chem. Commun.*, 1703-1704.
62. Kuciauskas, D., Liddell, P.A., Moore, T.A., Moore, A.L. and Gust, D. (1998) Solvent Effects and Electron Transfer Dynamics in a Porphyrin-Fullerene Dyad and a Carotenoporphyrin-Fullerene Triad., *Proc. Electrochem. Soc.* **8**, 242-261.
63. Imahori, H., Hagiwara, K., Aoki, M., Akiyama, T., Taniguchi, S., Okada, T., Shirakawa, M. and Sakata, Y. (1996) Linkage and Solvent Dependence of Photoinduced Electron Transfer in Zincporphyrin-C60 Dyads, *J. Am. Chem. Soc.* **118**, 11771-11782.
64. Imahori, H., Hagiwara, K., Akiyama, T., Aoki, M., Taniguchi, S., Okada, T., Shirakawa, M. and Sakata, Y. (1996) The Small Reorganization Energy of C_{60} in Electron Transfer, *Chem. Phys. Lett.* **263**, 545-550.
65.

66. Baran, P.S., Monaco, R.R., Khan, A.U., Schuster, D.I. and Wilson, S.R. (1997) Synthesis and Cation-Mediated Electronic Interactions of Two Novel Classes of Porphyrin-Fullerene Hybrids, *J. Am. Chem. Soc.* **119**, 8363-8364.
67. Safonov, I.G., Baran, P.S. and Schuster, D.I. (1997) Synthesis and Photophysics of a Novel Porphyrin-C_{60} Hybrid, *Tet. Lett.* **38**, 8133-8136.
68. McLean, A.J., McGarvey, D.J., Truscott, T.G., Lambert, C.R. and Land, E.J. (1990) Effect of Oxygen-Enhanced Intersystem Crossing on the Observed Efficiency of Formation of Singlet Oxygen, *J. Chem. Soc., Faraday Trans.* **86**, 3075-3080.
69. Schmidt, R. and Afshari, E. (1990) Effect of Solvent on the Phosphorescence Rate Constant of Singlet Molecular Oxygen, *J. Phys. Chem.* **94**, 4377-4378.
70. Baran, P.S. and Schuster, D.I. (1997), Unpublished results.
71. MacMahon, S.A., Schuster, D.I. and Guldi, D.M. (2001), Unpublished results.
72. Imahori, H., Cardoso, S., Tatman, D., Lin, S., Noss, L., Seely, G.R., Sereno, L., Chessa De Silber, J., Moore, T.A., Moore, A.L. and Gust, D. (1995) Photoinduced Electron Transfer in a Carotenobuckministerfullerene Dyad, *Photochem. Photobiol.* **62**, 1009-1014.
73. Williams, R.M., Zwier, J.M. and Verhoeven, J.W. (1995) Photoinduced Intramolecular Electron Transfer in a Bridged C_{60} (Acceptor)-Aniline (Donor) System; Photophysical Properties of the First "Active" Fullerene Diad, *J. Am. Chem. Soc.* **117**, 4093-4099.
74. Schuster, D.I., Cheng, P. and Guldi, D.M. (2000), Unpublished results.
75. Maggini, M., Guldi, D.M., Mondini, S., Scorrano, G., Paolucci, F., Ceroni, P. and Roffia, S. (1998) Photoinduced Electron Transfer in a Tris(2,2'-Bipyridine)-C_{60}-Ruthenium(II) Dyad: Evidence of Charge Recombination to a Fullerene Excited State, *Chem. Eur. J.* **4**, 1992-2000.
76. Fong II, R., Schuster, D.I. and Wilson, S.R. (1999) Synthesis and Photophysical Properties of Steriod-Linked Porphyrin-Fullerene Hybrids, *Org. Lett.* **1**, 729-732.
77. Fukuzumi, S., Ohkubo, K., Imahori, H., Shao, J., Ou, Z., Zheng, G., Chen, Y., Pandey, R.K., Fujitsuka, M., Ito, O. and Kadish, K.M. (2001) Photochemical and Electrochemical Properties of Zinc Chlorin-C_{60} Dyad as Compared to Corresponding Free-Base Chlorin-C_{60}, Free-Base Porphyrin-C_{60}, and Zinc Porphyrin-C_{60} Dyads, *J. Am. Chem. Soc.* **123**, 10676-10683.
78. Tkachenko, N.V., Rantala, L., Tauber, A.Y., Helaja, J., Hynninen, P.H. and Lemmetyinen, H. (1999) Photoinduced Electron Transfer in Phytochlorin-[60]Fullerene Dyads, *J. Am. Chem. Soc.* **121**, 9378-9387.
79. Imahori, H., Ozawa, S., Ushida, K., Takahashi, M., Azuma, T., Ajavakom, A., Akiyama, T., Hasegawa, M., Taniguchi, S., Okada, T. and Sakata, Y. (1999) Organic Photoelectrochemical Cell Mimicking Photoinduced Multistep Electron Transfer in Photosynthesis: Interfacial Structure and Photoelectrochemical Properties of Self-Assembled Monolayers of Porphyrin-Linked Fullerenes on Gold Electrodes, *Bull. Chem. Soc. Jpn.* **72**, 485-502.
80. Vehmanen, V., Tkachenko, N.V., Tauber, A.Y., Hynninen, P.H. and Lemmetyinen, H. (2001) Ultrafast Charge Transfer in Phytochlorin-[60]Fullerene Dyads: Influence of the Attachment Postion, *Chem. Phys. Lett.* **345**, 213-218.
81. Liddell, P.A., Kuciauskas, D., Sumida, J.P., Nash, B., Nguyen, D., Moore, A.L., Moore, T.A. and Gust, D. (1997) Photoinduced Charge Separation and Charge Recombination to a Triplet State in a Carotene-Porphyrin-Fullerene Triad, *J. Am. Chem. Soc.* **119**, 1400-1405.
82. Wasielewski, M.R. (1992) Photoinduced Electron Transfer in Supramolecular Systems for Artificial Photosynthesis, *Chem. Rev.* **92**, 435-461.
83. Connolly, J.S. and Bolton, J.R. (1988) in *Photoinduced Electron Transfer,* ed. M. Chanon, Elsevier, Amsterdam 303-393
84. Wasielewski, M.R., Gaines III, G.L., O'Neil, M.P., Svec, W.A., Niemczyk, M.P., Prodi, L. and Gosztola, D. (1992) in *Dynamics and Mechanisms of Photoinduced Transfer and Related Phenomena,* ed. H. Masuhara, Elsevier, New York 87-103
85. Carbonera, D., Valentin, M.D., Corvaja, C., Agostini, G., Giacometti, G., Liddell, P.A., Kuciauskas, D., Moore, A.L., Moore, T.A. and Gust, D. (1998) EPR Investigation of Photoinduced Radical Pair Formation and Decay to a Triplet State in a Carotene-Porphyrin-Fullerene Triad, *J. Am. Chem. Soc.* **120**, 4398-4405.
86. Kuciauskas, D., Liddell, P.A., Hung, S.-C., Lin, S., Stone, S., Seely, G.R., Moore, A.L., Moore, T.A. and Gust, D. (1997) Structural Effects on Photoinduced Electron Transfer in Carotenoid-Porphyrin-Quinone Triads, *J. Phys. Chem. B* **101**, 429-440.

87. Kuciauskas, D., Liddell, P.A., Moore, A.L., Moore, T.A. and Gust, D. (1998) Magnetic Switching of Charge Separation Lifetimes in Artificial Photosynthetic Reaction Centers, *J. Am. Chem. Soc.* **120**, 10880-10886.
88. Kuciauskas, D., Liddell, P.A., Lin, S., Stone, S.G., Moore, A.L., Moore, T.A. and Gust, D. (2000) Photoinduced Electron Transfer in Carotenoporphyrin-Fullerene Triads: Temperature and Solvent Effects, *J. Phys. Chem. B* **104**, 4307-4321.
89. Luo, C., Guldi, D.M., Imahori, H., Tamaki, K. and Sakata, Y. (2000) Sequential Energy and Electron Transfer in an Artificial Reaction Center: Formation of a Long-Lived Charge-Separated State, *J. Am. Chem. Soc.* **122**, 6535-6551.
90. Kuciauskas, D., Liddell, P.A., Lin, S., Johnson, T.E., Weghorn, S.J., Lindsey, J.S., Moore, A.L., Moore, T.A. and Gust, D. (1999) An Artificial Photosynthetic Antenna-Reaction Center Complex, *J. Am. Chem. Soc.* **121**, 8604-8614.
91. Gust, D. (2001), Private communication of unpublished results.
92. Deschenaux, R., Even, M. and Guillon, D. (1998) Liquid-Crystalline Mixed [60]Fullerene–Ferrocene Materials, *Chem. Commun.*, 537-538.
93. Dardel, B., Deschenaux, R., Even, M. and Serrano, E. (1999) Synthesis, Characterization, and Mesomorphic Properties of a Mixed [60]Fullerene-Ferrocene Liquid-Crystalline Dendrimer, *Macromoleules* **32**, 5193-5198.
94. Nierengarten, J.-F. (2000) Fullerodendrimers: A New Class of Compounds for Supramolecular Chemistry and Materials Science Applications, *Chem. Eur. J.* **6**, 3667-3670.
95. Imahori, H., Yamada, H., Nishimura, Y., Yamazaki, I. and Sakata, Y. (2000) Vectorial Multistep Electron Transfer at the Gold Electrodes Modified with Self-Assembled Monolayers of Ferrocene-Porphyrin-Fullerene Triads, *J. Phys. Chem. B* **104**, 2099-2108.
96. Imahori, H., Norieda, H., Yamada, H., Nishimura, Y., Yamazaki, I., Sakata, Y. and Fukuzumi, S. (2001) Light-Harvesting and Photocurrent Generation by Gold Electrodes Modified with Mixed Self-Assembled Monolayers of Boron-Dipyrrin and Ferrocene-Porphyrin-Fullerene Triad, *J. Am. Chem. Soc.* **123**, 100-110.
97. Guldi, D.M., Maggini, M., Menna, E., Scorrano, G., Ceroni, P., Marcaccio, M., Paolucci, F. and Roffia, S. (2001) A Photosensitizer Dinuclear Ruthenium Complex: Intramolecular Energy Transfer to a Covalently Linked Fullerene Acceptor, *Chem. Eur. J.* **7**, 1597-1605.
98. Luo, C., Guldi, D.M., Maggini, M., Menna, E., Mondini, S., Kotov, N.A. and Prato, M. (2000) Stepwise Assembled Photoactive Films Containing Donor-Linked Fullerenes, *Angew. Chem. Int. Ed. Engl.* **39**, 3905-09.
99. Segura, J.L., Gómez, R., Martín, N., Luo, C. and Guldi, D.M. (2001) Photoinduced Electron and Energy Transfer in C_{60}-based Conjugated Oligomer Containing Dyads and Triads, *Synth. Met.* **119**, 65-66.
100. Eckert, J.-F., Nicoud, J.-F., Nierengarten, J.-F., Liu, S.-G., Echegoyen, L., Barigelletti, F., Armaroli, N., Ouali, L., Krasnikov, V. and Hadziioannou, G. (2000) Fullerene-Oligophenylenevinylene Hybrids: Synthesis, Electronic Properties, and Incorporation in Photovoltaic Devices, *J. Am. Chem. Soc.* **122**, 7467-7479.
101. Armaroli, N., Barigelletti, F., Ceroni, P., Eckert, J.-F., Nicoud, J.-F. and Nierengarten, J.-F. (2000) Photoinduced Energy Transfer in a Fullerene–Oligophenylenevinylene Conjugate, *Chem. Commun.*, 599-600.
102. Matsumoto, K., Fujitsuka, M., Sato, T., Onodera, S. and Ito, O. (2000) Photoinduced Electron Transfer from Oligothiophenes/Polythiophene to Fullerenes (C_{60}/C_{70}) in Solution: Comprehensive Study by Nanosecond Laser Flash Photolysis Method, *J. Phys. Chem. B* **104**, 11632-11638.
103. Hal, P.A.v., Knol, J., Langeveld-Voss, B.M.W., Meskers, S.C.J., Hummelen, J.C. and Janssen, R.A.J. (2000) Photoinduced Energy and Electron Transfer in Fullerene-Oligothiophene-Fullerene Triads, *J. Phys. Chem. A* **104**, 5974-5988.
104. Hal, P.A.v., Janssen, R.A.J., Lanzani, G., Cerullo, G., Zavelani-Rossi, M. and Silvestri, S.D. (2001) Full Temporal Resolution of the Two-Step Photoinduced Energy-Electron Transfer in a Fullerene-Oligothiophene-Fullerene Triad Using Sub-10 fs Pump-Probe Spectroscopy, *Chem. Phys. Lett.* **345**, 33-38.
105. Lawson, G.E., Kitaygorodskiy, A. and Sun, Y.-P. (1999) Photoinduced Electron-Transfer Reactions of [60]Fullerene with Triethylamine, *J. Org. Chem.* **64**, 5913-5920.
106. Thomas, K.G., Biju, V., Guldi, D.M., Kamat, P.V. and George, M.V. (1999) Photoinduced Charge Separation and Stabilization in Clusters of a Fullerene-Aniline Dyad, *J. Phys. Chem. B* **103**, 8864-8869.

107. Kamat, P.V., Barazzouk, S., Hotchandani, S. and Thomas, K.G. (2000) Nanostructured Thin Films of C_{60}-Aniline Dyad Clusters: Electrodeposition, Charge Separation, and Photoelectrochemistry, *Chem. Eur. J.* **6**, 3914-3921.
108. Reed, C.A. and Bolskar, R.D. (2000) Discrete Fulleride Anions and Fullerenium Cations, *Chem. Rev.* **100**, 1075-1120.
109. Dubois, D., Kadish, K.M., Flanagan, S. and Wilson, L.J. (1991) Electrochemical Detection of Fulleronium and Highly Reduced Fulleride (C_{60}^{5-}) Ions in Solution, *J. Am. Chem. Soc.* **113**, 7773-7774.
110. Kato, T., Kodama, T., Shida, T., Nakagawa, T., Matsui, Y., Suzuki, S., Shiromaru, H., Yamauchi, K. and Achiba, Y. (1991) Electronic Absorption Spectra of the Radical Anions and Cations of Fullerenes: The Carbon Sixty-Atom and Seventy-Atom Molecules., *Chem. Phys. Lett.* **180**, 446-450.
111. Nonell, S., Arbogast, J.W. and Foote, C.S. (1992) Production of Fullerene (C_{60}) Radical Cation by Photosensitized Electron Transfer, *J. Phys. Chem.* **96**, 4169-4170.
112. Lem, G., Schuster, D.I., Courtney, S.H., Lu, Q. and Wilson, S.R. (1995) Addition of Alcohols and Hydrocarbons to Fullerenes by Photosensitized Electron Transfer, *J. Am. Chem. Soc.* **117**, 554-555.
113. Reed, C.A., Kim, K.-C., Bolskar, R.D. and Mueller, L.J. (2000) Taming Superacids: Stabilization of the Fullerene Cations HC_{60}^{+} and C_{60}^{+}, *Science* **289**, 101-104.
114. Fukuzumi, S., Mori, H., Imahori, H., Suenobu, T., Araki, Y., Ito, O. and Kadish, K.M. (2001) Scandium Ion-Promoted Photoinduced Electron-Transfer Oxidation of Fullerenes and Derivatives by p-Chloranil and p-Benzoquinone, *J. Am. Chem. Soc.* **123**, 12458-12465.
115. Steinberg-Yfrach, G., Rigaud, J.-L., Durantini, E.N., Moore, A.L., Gust, D. and Moore, T.A. (1998) Light-Driven Production of ATP Catalysed by F_0F_1-ATP Synthase in an Artificial Photosynthetic Membrane, *Nature* **392**, 479-482.
116. Fukuzumi, S., Imahori, H., Okamoto, K., Yamada, H., Fujitsuka, M., Ito, O. and Guldi, D.M. (2001) Uphill Photooxidation of NADH Analogues by Hexyl Viologen Catalyzed by Zinc Porphyrin-Linked Fullerenes, *J. Phys. Chem. A*, in press.